

國立交通大學

統計學研究所

碩士論文

計算統計方法在積體電路設計最佳化及敏感度分析之研究

Computational Statistics Approach to Integrated Circuit
Design Optimization and Sensitivity Analysis

研究生：羅婉文

指導教授：洪慧念 博士

李義明 博士

中華民國九十五年七月



計算統計方法在積體電路設計最佳化及敏感度分析之研究

Computational Statistics Approach to Integrated Circuit Design Optimization
and Sensitivity Analysis

研究生：羅婉文

Student : Wan-Wen Lo

指導教授：洪慧念 博士

Advisor : Dr. Hui-Nien Hung

李義明 博士

Advisor : Dr. Yiming Li

國立交通大學



A Thesis

Submitted to the Department of Statistics

National Chiao Tung University

in partial Fulfillment of the Requirements

for the Degree of

Master

in

Statistics

July 2006

Hsinchu, Taiwan

中華民國九十五年七月



© Copyright by Wan-Wen Lo 2006

All Rights Reserved





計算統計方法在積體電路設計最佳化及敏感度分析之研究

學生：羅婉文

指導教授：洪慧念 博士
李義明 博士

國立交通大學 統計研究所 碩士班

摘 要

現今電子產品中，為了滿足民生或工業消費上的需求，設計上須達到特定之商業規格，其中積體電路(ICs)在電子產業中扮演著重要角色與地位，要如何將積體電路設計達到想要的規格，通常設計者必須調整其中的主、被動元件以及積體電路佈局等參數，使得電氣規格可以達到我們想要的設計目標。要如何掌握電路行為的趨勢來符合嚴格的需求是現今市場競爭上困難的一件事，傳統上為了滿足工程需求，工程師往往反覆不斷的手動調整係數與執行電路模擬器，才能找出一組可行的參數組合來達到想要的設計結果；或者用數值最佳化的方法、演化式生物計算工程的方法、蒙地卡羅的方法設計參數，這些方法各有其優缺點。本論文嘗試提出一個整合電路模擬器與實驗設計的計算統計方法應用在積體電路的設計最佳化與規格敏感度分析，我們利用此方法研究類比與數位電路之設計問題展現出不錯的結果。

藉由此系統化的方法，首先應用在由 0.25 微米金屬氧化物半導體場效應電晶體所組成之低雜訊放大器射頻積體電路設計。例如，若我們所討論的電路特性希望規格為：一、輸入反射損失小於-10dB；二、輸出反射損失小於-10dB；三、輸入端與輸出端隔離度小於-25dB；四、輸出增益望大；五、穩定因子大於 1；六、雜訊指數小於 2；七、第三階截斷點(IIP3)大於-10。藉由呼叫電路模擬器取得電路特性，吾人首先透過篩選實驗，十個顯著的電路參數由 13 個參數中被挑選出來做進一步的中央合成設計，進而導出各電路特性相對應的二次反應曲面模型，同時使用望想函數(desirability function)，吾人可取得最佳解；若電路特性未達到希望的規格，可適當的調整參數範圍，最後使得

所研究的電路特性達到所預期的規格範圍內。同時由取得最佳解之敏感度分析，得知我們所估算的參數組合對電路特性是穩定的。

另外，吾人也進一步將此方法應用在數位電路的性能敏感度分析上，例如由 65 奈米金屬氧化物半導體場效應電晶體所組成之靜態隨機讀取記憶體之靜態雜訊邊際(static noise margin)敏感度分析，將靜態隨機讀取記憶體分成六個電晶體組態與四個電晶體組態討論，我們希望靜態雜訊邊際的變異越小越好。將這兩種結構以 10% 元件長度與偏壓當作三個標準差來探討其變異，分析出六個電晶體組態與四個電晶體組態的靜態雜訊邊際落在我們測試的條件準則下達 98% 和 95.8%，相較之下六個電晶體組態的靜態雜訊邊際來的穩定。

總之，藉由以上的例子，吾人歸結得知，此有系統的計算統計方法，初步研究結果顯示，它可以成功的應用在類比與數位積體電路的設計上，且都有不錯的設計穩定性。吾人深信此統計方法可進一步推廣，適當地用在積體電路設計最佳化，並量化分析電路的操作特性與可靠度之變化趨勢，進而有效解決不同電路的設計問題。



Computational Statistics Approach to Integrated Circuit Design Optimization and Sensitivity Analysis

Student : Wan-Wen Lo

Advisor : Dr. Hui-Nien Hung
Dr. Yiming Li

Institute of Statistics
National Chiao Tung University

Abstract

It is known that integrated circuits (ICs) design nowadays plays a crucial role for microelectronics industry; in particular, for highly competitive consumer products. To meet specified electrical characteristics and performance of designed product, designer in general has to tune parameters of the passive and active devices ranging from resistors, capacitors, inductors, line width, line length, to transistor size, etc. Diverse approaches have been proposed to reduce products' designing cycles and accelerate time to market. These methods include (1) directly empirical procedure, (2) numerical optimization technique, (3) evolutionary algorithm, and (4) Monte Carlo statistical method, and have demonstrated their merit and validity. We believe that a systematical integration of circuit simulation tool, design of experiment, and response surface model may provide an alternative way to advanced IC design optimization and sensitivity analysis of performance.

In this thesis, by verifying two different analog and digital circuits, a low noise amplifier and static random access memory, we develop a computational statistics approach, which is mainly based upon SPICE circuit simulator, a screen design, a central composite design (CCD), and a 2nd order response surface model (RSM). We firstly state the computational algorithm by taking a low noise amplifier circuit with 0.25 μm MOSFETs as an example. The circuit specification consists of (1) the input return loss < -10 dB, (2) the output return loss < -10 dB, (3) reverse isolation < -25 dB, (4) voltage gain which is as great as possible, (5) stability factor > 1 , (6) noise figure < 2 dB, and (7) the third-order-intercept point > -10 dB. To achieve the aforementioned

seven circuit specifications, calling circuit simulator to obtain circuit performances is performed and then ten significant results among thirteen parameters are selected from the screening design. By simultaneously running SPICE circuit simulator, a ten-parameter face centered cube design is then performed in the step of central composite design. We use the 149 simulation results in constructing the corresponding 2nd order response surface model (it is a 10-variable 2nd order polynomial) by using statistical software, Design Expert®. We note that, for validating the constructed model, the model adequacy checking and the accuracy verification are necessary. If the model adequacy checking fails, we transform the circuit performance by BOX-COX transformation. Furthermore, adjustment of parameters' range corresponding to the circuit specification will be enabled for accuracy verification. With the 2nd order RSM, design optimization and sensitivity analysis of performance will be explored. For the design optimization, if one of the circuit performances does not meet its specification, we adjust the parameter range corresponding to the circuit specification, and return to the step of CCD. If the optimized results are eventually satisfied the aforementioned seven specifications, the first three optimal recipes will be provided. Performance sensitivity with respect to certain optimized parameter (or all parameters) is investigated by using RSM to an optimized recipe with 100 randomly generated normal samples. The optimized recipe is right the mean of the normal distribution; and one per centum of the optimized recipe is assumed to be the standard deviation. Our result shows that the optimized recipe is stable to the circuit performance. Similar methodology is further applied to explore the variation of static noise margin (SNM) of six- and four-transistors (6T and 4T) static random access memory (SRAM) cells with respect to channel length and supply voltage. For SRAM with 65 nm CMOS devices, our result shows that 98 % (theoretically it should be 100 %) variation of SNM is within 3-sigma for the 6T SRAM with 3-sigma variation of parameters. It is better than that of the result of 4T SRAM (95.8 %). Thus, it quantitatively confirms that SRAM with 6T configuration is more stable than it with 4T configuration.

In conclusion, we systematically implement a computational statistics approach to ICs' design optimization and sensitivity analysis. Successful application of the method to study analog and digital circuits shows its computational efficiency and engineering accuracy, compared with large-scale SPICE circuit simulations. This approach is suitable for optimization problems and diagnosis of quantify trade-offs in IC industry.

誌 謝

這份論文能夠順利完成，首先感謝 洪慧念教授給予學生最大自由度，讓學生可以完成感興趣的研究，感謝洪老師在課業以及生活上的鼓勵及支持。其次，學生感謝指導老師 李義明副教授，感謝恩師兩年來指導學生論文方向脈絡，研究方法之傳授及論文撰寫之推敲斟酌，讓學生研究能力之激發有深厚的影響。恩師學術研究態度嚴謹，在半導體數學模式及電腦模擬計算之專業知識，足以為學生日後之表率。學生在此謹獻上最誠摯的感謝與敬意。

另外感謝 許文郁老師、彭松村老師來當學生的口試委員，讓學生的論文可以更加完備，更符合統計和工程雙方面的觀點。

在平行與科學計算實驗室方面，我要感謝周宏穆學長、建松、孟家學弟撥空教我積體電路上的觀念，真的讓我獲益匪淺；感謝卓彥羽學長百忙之中在程式上的協助，真的解決了我很多困難；紹銘學長、陳璞學長、傳盛學長、正凱學長總是無條件的當我論文問題的求救對象。景嵐學長、煒昕、柏賢，宏榮加上東祐學弟在此一並感謝。

統研所方面，感謝沛君、謝宛茹、孟樺、秀慧、鶯筑、張宛茹、耀文、泓毅；因為有你們的關心，帶給我歡樂，替我加油打氣，謝謝你們平常聽我發牢騷，有你們這一群朋友真的很榮幸。統研所是一個很溫馨的地方，讓我總是笑嘻嘻的與你們玩在一起。

我還要感謝我的好朋友們，運璿、怡婷、勇志、千姿、其沛，瑾魚，穎劭學姐總是在我徬徨失措的時候給我許多建議，有時半夜接到我騷擾的電話還陪我講講話，真的很感謝你們，有你們的相伴覺得很幸福。

最後最應該感謝的是我的爸爸，媽媽，和我的哥哥姐姐以及景偉，週末回家總是讓我感覺家的溫馨，不用煩惱任何家裡的事情，讓我得到最充裕的休息，再重新出發，也因為你們的關心與支持讓我勇敢的在外面闖蕩，現在終於完成論文畢業了，真的很感謝你們。

感謝這段期間大家對我的包容、關懷與愛護。這篇論文，這個工作，以及我在交大的一切成長，沒有你們，是完全沒有辦法達成的，一切的功勞都歸因於全部的人。謝謝大家一直挺我鼓勵我，使我順順利利的度過這段非凡且精采的日子。

本論文感謝行政院國家科學委員會(計畫編號 NSC-93-2115-E-492-008、NSC-94-2115-E-009-084)、卓越延續計畫(計畫編號 NSC-94-2752-E-009-003-PAE、NSC-95-2752-E-009-003-PAE)、五年五百億計畫、經濟部科專計劃(計畫編號 93-EC-17-A-07-S1-0011)及台灣積體電路製造股份有限公司 2005~2006 年研究計畫之資助。

在此將這篇論文獻給所有關心我以及我所愛的人，謝謝你們。

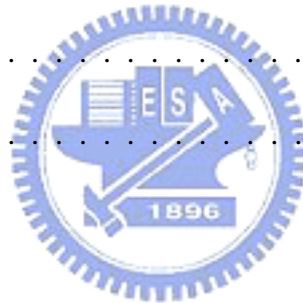
羅婉文 謹誌

中華民國九十五年七月三十一日 于風城交大



Contents

Abstract (in Chinese)	v
Abstract (in English)	vii
Acknowledgments	ix
List of Tables	xvi
List of Figures	xxi
1 Introduction	1
1.1 Motivation	3
1.2 Literature Review	4
1.3 Objectives	6
1.4 Outline of the Thesis	7
2 Statistical Methodology	8
2.1 Screening Design	10



2.2	Central Composite Design	11
2.3	Models Construction	13
2.4	Variable Selection	18
2.5	Model Adequacy Checking	24
2.6	Desirability Function	26
2.7	Other Design Methods	31
2.7.1	Taguchi Method	31
2.7.2	Mixture Design	32
2.7.3	Comparison with the Popular Designs	32
2.8	Summary	33
3	Low Noise Amplifier	35
3.1	A LNA Circuit with Deep Submicron MOSFETs	35
3.1.1	Noise Figure	37
3.1.2	Stability Factor	39
3.2	Linearity	40
3.3	Problem Description	41
3.4	Circuit Simulators	42
3.5	Summary	43
4	Results of DOE for LNA Circuit	45



4.1	Results of The Screening Design	45
4.1.1	The Fractional Factorial Design	46
4.1.2	Summary	47
4.2	Results of The Central Composite Design	58
4.2.1	The Face Centered Cube Design	58
4.2.2	The Response Surface Model	61
4.2.3	Summary	67
4.3	Model Adequacy Checking	67
4.3.1	Summary	77
4.4	Accuracy Verification	77
4.4.1	Accuracy Verification Results	77
4.4.2	Summary	78
5	LNA Circuit Design Optimization	84
5.1	Optimization Results Using the Stepwise Regression Models	86
5.2	Comparison of Three Optimized Cases	95
5.3	Summary	105
6	Sensitivity Analysis of the Optimized LNA Specification	106
6.1	Sensitivity Analysis for LNA Circuit	107
6.2	Summary	113

7	Application to Static Random Access Memory Cell	114
7.1	The 6T SRAM Cells	114
7.2	The 4T SRAM Cells	116
7.3	The DOE of 6T and 4T SRAM Cells	117
7.3.1	The Response Surface Model for 6T and 4T SRAM Cells	118
7.3.2	Model Adequacy Checking for 6T and 4T SRAM Cells	119
7.3.3	Accuracy Verification for 6T and 4T SRAM Cells	120
7.4	The Sensitivity Analysis for 6T and 4T SRAM Cells	124
7.5	Summary	125
8	Conclusions and Future Work	127
8.1	Conclusions	128
8.2	Suggestions to Future Work	130
	References	131
 Appendix A		
	Contour Plots of the Optimal Recipe for the CCF Design	139
 Appendix B		
	Netlist of LNA Circuit	162
 Appendix C		



Netlist of SRAM Cells 166

Appendix D

A Example of Design Expert 6.0.6 169

Appendix E

Sensitivity Analysis by Varying Ten Factors for the LNA Circuit 188



List of Tables

2.1	Difference between Taguchi approach and classical DOE.	33
4.1	The levels of screening design for the 13 factors.	48
4.2	A list of the results for the screening design, where "1" means the most important term with respect to the corresponding response.	49
4.3	The minimum and maximum of seven responses in the six settings of Load. The Load factor is 4.5 which makes the voltage gain close to our target. . .	50
4.4	A list of the results of the predicted values after optimization in the first three experiments using CCF design.	59
4.5	Experiment levels for 10 factors after optimization of the 3th experiment . .	60
4.6	The information of 7 response surface models for the LNA circuit using CCF design.	62

4.7	The information of the 5 response surface models and 2 transformed response surface models for the LNA circuit using CCF design with stepwise regression method.	62
4.8	The coefficients of $1/S_{11}$ with coded factors in a significance order of the stepwise regression.	63
4.9	The coefficients of S_{12} with coded factors in a significance order of the stepwise regression.	63
4.10	The coefficients of S_{21} with coded factors in a significance order of the stepwise regression.	64
4.11	The coefficients of S_{22} with coded factors in a significance order of the stepwise regression.	64
4.12	The coefficients of K with coded factors in a significance order of the stepwise regression.	65
4.13	The coefficients of NF with coded factors in a significance order of the stepwise regression.	65
4.14	The coefficients of $IIP3$ with coded factors in a significance order of the stepwise regression.	66
4.15	Accuracy verification of the results calculated from the constructed response surface model.	78

4.16	Accuracy verification of the results obtained from circuit simulator.	79
5.1	The constraints of LNA circuit parameters.	85
5.2	The targets of responses.	85
5.3	The constraint for the case of satisfied all specifications. We modify the specifications within $2\hat{\sigma}$	87
5.4	The constraint for the case of minimized noise figure. We modify the specifications within $2\hat{\sigma}$	88
5.5	The constraint for the case of maximized voltage gain. We modify the specifications within $2\hat{\sigma}$	88
5.6	Optimal recipes for the case of satisfied all specifications calculated by the 2^{nd} order response surface model. "1" means the highest priority.	89
5.7	Optimal recipes for the case of minimized noise figure calculated by the 2^{nd} order response surface model. "1" means the highest priority.	90
5.8	Optimal recipes for the case of maximized voltage gain calculated by the 2^{nd} order response surface model. "1" means the highest priority.	91
5.9	Optimal results for the case of satisfied all specifications calculated by the 2^{nd} order response surface model. "1" means the highest priority.	92
5.10	Optimal results for the case of minimized noise figure calculated by the 2^{nd} order response surface model. "1" means the highest priority.	92

5.11	Optimal results for the case of maximized voltage gain calculated by the 2 nd order response surface model. "1" means the highest priority.	93
5.12	Optimal results for the case of satisfied all specifications by running circuit simulator. "1" means the highest priority.	93
5.13	Optimal results for the case of minimized noise figure by running circuit simulator. "1" means the highest priority.	94
5.14	Optimal results for the case of maximized voltage gain by running circuit simulator. "1" means the highest priority.	94
6.1	Sensitivity analysis for LNA circuit calculated from the response surface model which is obtained from circuit simulator by varying VB1. Calculated mean and standard deviation for seven circuit performances are shown. . . .	108
6.2	Sensitivity analysis for LNA circuit calculated from response surface models and obtained from circuit simulator by varied 10 factors, displaying calculated mean and standard deviation for seven circuit performances. . . .	109
7.1	The levels of each factor for 6T and 4T SRAM cells	118
7.2	The calculated results of SNM response surface model for the 6T and 4T SRAM cells using CCF design.	119

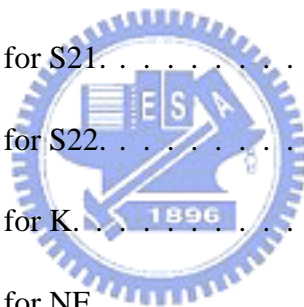
- 7.3 Accuracy verification of the response values calculated from the response surface model and obtained from circuit simulator for 6T and 4T SRAM cells. 121
- 7.4 Comparison of the sensitivity of the SNM for 6T SRAM cell between the sensitivity of the SNM for 4T SRAM cell. The mean of L_1 , L_2 , and L_3 is set to be its nominal values 65 nm, respectively; and VDD is set to be its nominal value 1.2 V. The standard deviation is 3.3 % for each nominal value. We generate 500 normally and independently distributed pseudo-random numbers for these four parameters. 125



List of Figures

2.1	The proposed main computational procedure for IC design optimization in this work.	9
2.2	A central composite design of two factors.	14
2.3	Comparison of the three types of central composite designs.	14
2.4	A flowchart of the stepwise regression algorithm used in our work.	23
2.5	An example of residual normal probability plot.	29
2.6	An example of scatter plot of predicted values versus residuals.	29
2.7	Individual desirability functions for the simultaneous optimization.	30
3.1	The explored LNA circuit in our experiment.	37
3.2	An illustration of spurious-free dynamic range with the noise floor and IIP3.	41
3.3	A flow of circuit simulation.	43
3.4	A RF model applied in this work.	44
4.1	A half-normal plot for the effect of S11.	51

4.2	A half-normal plot for the effect of S12.	52
4.3	A half-normal plot for the effect of S21.	53
4.4	A half-normal plot for the effect of S22.	54
4.5	A half-normal plot for the effect of K.	55
4.6	A half-normal plot for the effect of NF.	56
4.7	A half-normal plot for the effect of IIP3.	57
4.8	Residual normal probability plots for (a) S11 and (b) 1/S11.	68
4.9	Residual scatter plots for (a) S11 and (b) 1/S11.	69
4.10	A model adequacy checking for S12.	70
4.11	A model adequacy checking for S21.	71
4.12	A model adequacy checking for S22.	72
4.13	A model adequacy checking for K.	73
4.14	A model adequacy checking for NF.	74
4.15	Residual normal probability plots for (a) IIP3 and (b) $\log(IIP3 + 11.1265)$	75
4.16	Residual scatter plots for (a) IIP3 and (b) $\log(IIP3 + 11.1265)$	76
4.17	A scatter plot calculated from the response surface model versus values obtained from circuit simulator for S11.	79
4.18	A scatter plot calculated from the response surface model versus values obtained from circuit simulator for S12.	80



4.19	A scatter plot calculated from the response surface model versus values obtained from circuit simulator for S21.	80
4.20	A scatter plot calculated from the response surface model versus values obtained from circuit simulator for S22.	81
4.21	A scatter plot calculated from the response surface model versus values obtained from circuit simulator for K.	81
4.22	A scatter plot calculated from the response surface model versus values obtained from circuit simulator for NF.	82
4.23	The scatter plots of values calculated from response surface models versus values obtained from circuit simulator for IIP3.	83
5.1	Comparison of original case and three optimized cases for the result of S11 response. A zoom-in plot for the operation frequency.	97
5.2	Comparison of original case and three optimized cases for the result of S12 response. A zoom-in plot for the operation frequency.	98
5.3	[Comparison of original case and three optimized cases for the result of S21 response. A zoom-in plot for the operation frequency.	99
5.4	Comparison of original case and three optimized cases for the result of S22 response. A zoom-in plot for the operation frequency.	100

5.5 Comparison of original case and three optimized cases for the result of K response. A zoom-in plot for the operation frequency. 101

5.6 Comparison of original case and three optimized cases for the result of NF response. A zoom-in plot for the operation frequency. 102

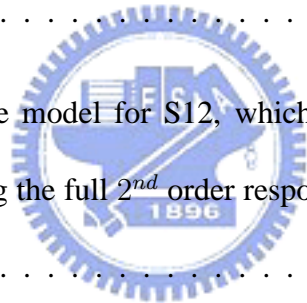
5.7 Comparison of original case and three optimized cases for the result of IIP3 response. A zoom-in plot for the operation frequency. 104

6.1 Statistical distribution of the model for S11, which is calculated by the sensitivity analysis and using the full 2nd order response surface model by varying VB1. 109

6.2 Statistical distribution of the model for S12, which is calculated by the sensitivity analysis and using the full 2nd order response surface model by varying VB1. 110

6.3 Statistical distribution of the model for S21, which is calculated by the sensitivity analysis and using the full 2nd order response surface model by varying VB1. 110

6.4 Statistical distribution of the model for S22, which is calculated by the sensitivity analysis and using the full 2nd order response surface model by varying VB1. 111



6.5	Statistical distribution of the model for K, which is calculated by the sensitivity analysis and using the full 2^{nd} order response surface model by varying VB1.	111
6.6	Statistical distribution of the model for NF, which is calculated by the sensitivity analysis and using the full 2^{nd} order response surface model by varying VB1.	112
6.7	Statistical distribution of the model for IIP3, which is calculated by the sensitivity analysis and using the full 2^{nd} order response surface model by varying VB1.	112
7.1	A circuit of 6T SRAM cell used in our circuit simulation.	116
7.2	A circuit of 4T SRAM cell used in our circuit simulation.	117
7.3	A 3D plot of SNM for 6T and 4T SRAM cells with respect to L_1 and L_2	120
7.4	A model adequacy checking for 6T and 4T SRAM cells.	122
7.5	A scatter plot calculated from the response surface model versus values obtained from the circuit simulator.	123
7.6	A comparison of the sensitivity of SNM for 6T SRAM cell and the sensitivity of SNM for 4T SRAM cell.	126
A.1	Contour plots of the optimal recipe for the CCF Design.	161

E.1 Statistical distribution of the model for S11, which is calculated by the sensitivity analysis and using the full 2^{nd} order response surface model by varying 10 factors. 189

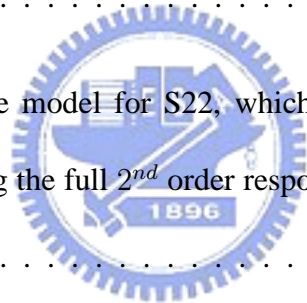
E.2 Statistical distribution of the model for S12, which is calculated by the sensitivity analysis and using the full 2^{nd} order response surface model by varying 10 factors. 189

E.3 Statistical distribution of the model for S21, which is calculated by the sensitivity analysis and using the full 2^{nd} order response surface model by varying 10 factors. 190

E.4 Statistical distribution of the model for S22, which is calculated by the sensitivity analysis and using the full 2^{nd} order response surface model by varying 10 factors. 190

E.5 Statistical distribution of the model for K, which is calculated by the sensitivity analysis and using the full 2^{nd} order response surface model by varying 10 factors. 191

E.6 Statistical distribution of the model for NF, which is calculated by the sensitivity analysis and using the full 2^{nd} order response surface model by varying 10 factors. 191



E.7 Statistical distribution of the model for IIP3, which is calculated by the sensitivity analysis and using the full 2nd order response surface model by varying 10 factors. 192





Chapter 1

Introduction



Integrated circuits (ICs) market has become so intense that designers have adopted various optimization strategies in an effort to reduce the development time and to improve circuit performance. It is increasingly important to design robust circuits that would minimize fluctuations of the circuit performance. Designers usually do many try-and-error experiments to achieve specifications. One common practice is to guess the improved settings of the control factors using engineering judgment, and then conducts a paired comparison with the starting conditions. The guess-and-test cycle is repeated until an improvement has been obtained, the deadline has been reached, or the budget has been exhausted. This practice relies heavily on luck. It is inefficient and time-consuming [1].

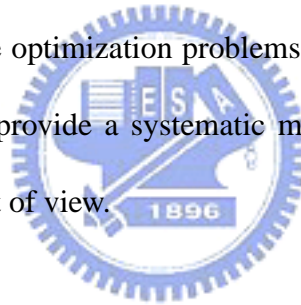
Due to the excessive time and high costs associated with physical experiments, designers have applied Simulation Program with Integrated Circuit Emphasis (SPICE) to simulate the circuit performance and predict the circuit characteristics. Different computational methods together with the circuit simulation tools to achieve optimization and sensitivity analysis have been of great interests.

In this thesis, a statistical approach is systematically developed for the circuit optimization and the sensitivity analysis in the low noise amplifier (LNA) and static random access memory circuit carried out as examples. Based on the screening design, the central composite design, a SPICE simulator, the response surface model, and the optimization using desirability function, the circuit performances have been optimized with respect to different specified constraints. For example, for the studied LNA circuit, they are (1) shifting the input return loss (S11) to the specific target; (2) shifting the output return loss (S22) to the specific target; (3) shifting the reverse isolation (S12) to the specific target; (4) maximizing the voltage gain (S21); (5) moving the stability factor (K) to the specific target; (6) moving the noise figure (NF) to the specific target; and (7) moving the third order intercept point (IIP3) to the specific target. Furthermore, the statistical approach also applies systematically to 6T and 4T static random access memory (SRAM) cells and we investigate the sensitivity of the static noise margin (SNM) for 4T and 6T SRAM cells.

1.1 Motivation

When circuit designers encounter the optimization problem, they often solve it according to their experiences. However, to extract a proper parameter setting of the VLSI circuit is a difficult problem and the empirical knowledge is needed [2][3][4][5][6]. If the circuit designers set the parameters corresponding to the experiences based on empirical formulas, an optimization procedure is needed to loop for times to get acceptable results.

So far, many researches have pointed out the methodologies for digital circuit optimization. Those methodologies are based on conventional optimization techniques which are in turn based on developed various local solution properties and they are ineffective or lack of accuracy [7][8][9][10]. These optimization problems often appear with high-dimensional and nonlinear state, and we provide a systematic method to explore this problem from computational statistical point of view.



1.2 Literature Review

Generally speaking, there are four types of optimization approaches: the brute force method, numerical optimization method, evolutionary algorithm method, and Monte Carlo statistical method. We discuss each method in brief.

(1) Brute force method

Brute force method is a traditional method for solving problem. This is a method that we try each possible solution one by one when we can not find the solution directly.

(2) Numerical optimization method

The Gauss-Newton method, for example, is a basic algorithm for solving nonlinear optimization problem, and Levenberg-Marquardt (LM) method is a quasi-Newton method to accelerate the Gauss-Newton method [16][17][18]. They start with an initial guess, and follow the direction of the normal of the gradient to find the optimal solution.

(3) Evolutionary algorithm method

Genetic algorithm (GA), for example, is a global search algorithm based on Darwinian survival of the fittest approach [19]. It has been proved having a capability of domain independent [20] and is an effective search method for large space problem [21]. The method could be adopted in many fields, such as combinatorial and numerical optimizations [22], supervised and unsupervised learning [23], and molecular computing [24]. In microelectronics, many works had been done on various VLSI circuit designs, such as cell placement

[25], channel routing [26], and model parameters extraction [27].

In addition, neural network (NN) is an artificial intelligent algorithm that mimics the behavior of human brain firstly established by McCulloch and Pitts in 1943. This model was first considered to be binary devices with fixed thresholds which is able to perform simple logic, such as unit and intersection. Currently NN has been widely used in digital signal processing, such as eigen-state problem [29], image process, audio pattern recognition [30], and feature classification. Due to the strong capability, there are some research using NN for solving numerical problem like ordinary/partial differential equations [31] and other numerical methods [32]. Moreover, it is also applied in parameters extraction [33].

(4) Monte Carlo statistical method

Statistical simulation methods may be contrasted to conventional numerical discretization methods, which typically are applied to ordinary or partial differential equations that describe some underlying physical or mathematical system. In many applications of Monte Carlo, the physical process is simulated directly, and there is no need to even write down the differential equations that describe the behavior of the system. The only requirement is that the physical (or mathematical) system be described by probability density functions [34][35].

Comparison among these methods, the brute force method is more ineffective than

others, but is a basic and direct method. Traditional numerical method like LM method that is necessary for a good initial value and easily trapped into local optima. However, compared with the global optimization technique such as genetic algorithm method, the LM method finds a solution rapidly.

1.3 Objectives

In this work, we will provide a computational statistical methodology to study the specification problem of circuits. We take a popular used circuit, such as low noise amplifier (LNA) circuit as be an example firstly. Here we want to optimize seven circuit performances to each specific value: (1) input return loss (S11); (2) output return loss (S22); (3) reverse isolation (S12); (4) voltage gain (S21); (5) stability factor (K); (6) noise figure (NF); and (7) the third order intercept point (IIP3). The object of this work is trying to construct the response surface model and to obtain the optimal recipes. In our process of the methodology, we verify the response surface models which are the relation of circuit parameters and circuit performance, then the model will reflect realistic circuit performance. Furthermore, by using desirability function with seven performance constraints supplies us optimal solutions. Finally, we perform the sensitivity analysis with the constructed model, they help us understand whether the distribution of the seven circuit performances are in their specific values that we assigned. Our second application is 6T and 4T SRAM cells.

We construct the response surface models and investigate the sensitivity of the SNM for 6T and 4T SRAM cells.

1.4 Outline of the Thesis

This thesis is organized as follows. In Chap. 2, the statistic methodology and the procedure of methodology in this work will be introduced in detail. The application of the statistical method to a low noise amplifier will be discussed in Chap. 3. The results of design of experiment which contain screening design, central composite design, construction of response surface model, model checking, and accuracy verification are shown in Chap. 4. The three optimized cases which are satisfied all specifications, minimized noise figure, and maximized voltage gain are provided in Chap. 5. Finally the outcomes of the LNA circuit sensitivity analysis have been shown in Chap. 6. The other application of the statistical method to static random access memory will be discussed in Chap. 7. Finally we draw conclusions and suggest future work.

Chapter 2

Statistical Methodology

In this chapter, we introduce the content of main methodology developed in this work in the following sections. A methodology flow is shown in Fig. 2.1, and then two designs will be discussed. First, screening design, in this step we merely use fewer experiments for screening the most important factors of the circuit parameters. After determining the important factors, we will execute the other design, central composite design. Next we construct the response surface models which are used to find the parameters to optimize circuit performance. In addition, we will describe some related applications of this work.

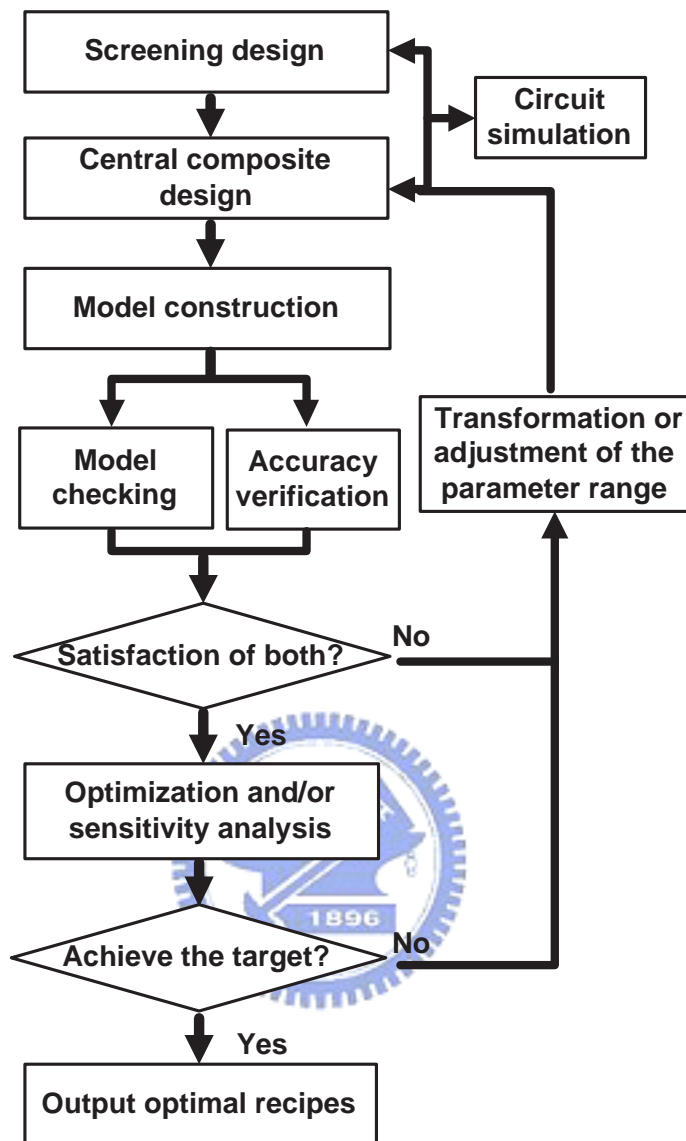


Figure 2.1: The proposed main computational procedure for IC design optimization in this work. First we use fewer experiments to select the important factors by screening design. Then we execute central composite design and construct model. The model adequacy checking is necessary to check the model assumption, and the accuracy verification is to check the values that we are interested in the accuracy of the model within our high and low level settings. Finally, we use the model for optimization or sensitivity analysis. If we don't achieve the target we will adjust the parameter range and repeat the flow chart which restarts at the step of central composite design

2.1 Screening Design

Screening design usually leads to an experiment which is designed to investigate these factors with a view toward eliminating some unimportant ones. In other words, we determine significant factors by screening design. To determine factor's significance, two-level fractional factorial design or Plackett-Burman design is ideally suited for screening design [36]. In short, screening designs are economically experimental plans that focus on determining the relative significance of many main effects with resolution III or IV (but the designs of this case require more runs than a resolution III design) [36].

Two-level fractional factorial design can reasonably assume that high-order interactions are negligible. We can run only a fraction of the complete factorial experiment to obtain information on the main effects and low-order interactions. For example, in one-half fraction of the 2^3 design (2^{3-1} design), A and BC are aliases, B and AC are aliases, C and AB are aliases, where A , B , and C are factors. When designs with resolution III, main effects are aliases with two-factor interactions and two-factor interactions may be aliased with each other. Sometimes designs with resolution IV are also used for screening designs. In this design main effects are aliased with, at worst, three-factor interactions. This is better from the confounding viewpoint, but the designs require more runs than a resolution III design.

Plackett-Burman design, attributed to Plackett and Burman (1946) [37], is two-level fractional designs for studying up to $k = N - 1$ variables in N runs, where N is a multiple

of 4. In a Plackett-Burman design, main effects are heavily confounded with two-factor interactions in general. For example, $N = 12$, every main effect is partially aliased with every two-factor interaction. Each main effect is partially aliased with 45 two-factor interactions.

And the plus and minus signs are:

$$K = 11, N = 12 \quad + + - + + + - - - + - . \quad (2.1)$$

When we analyze data from screening designs, the use of an error mean square obtained by pooling high order interactions is inappropriate occasionally. To overcome this problem a half-normal probability plot of the estimates of the effects is suggested. The half-normal plot consists of the point:

$$(\Phi^{-1}(0.5 + 0.5[i - 0.5]/I), |\hat{\theta}|_{(i)}), \quad (2.2)$$

for $i = 1, \dots, I$. The Φ is the cumulated density function of the standard normal distribution. If factors are unimportant, the effects with mean zero and variance σ^2 will tend to fall along a straight line on this plot, whereas important factors will not lie along the straight line [38].

2.2 Central Composite Design

The central-composite design (CCD) is perhaps the most common experimental design used to generate second-order response models. These designs combine a two-level full factorial or fractional factorial design of n_f runs with $2k$ axial runs and n_c center runs

to estimate curvature, where k represents the number of control factors [38]. Figure 2.2 illustrates a CCD for two factors. The axial points represent new extreme values for each factor in the design. There is three varieties of CCD which are CCC, CCI, and CCF.

The central composite circumscribed (CCC) designs are the original form of the central composite design. The axial points at some distance α from the center is based on the properties desired for the design and the number of factors in the design. The axial points establish new extremes for the low and high settings for all factors. Figure 2.3 illustrates a CCC design. These designs have circular, spherical, or hyperspherical symmetry and require 5 levels for each factor. Augmenting an existing factorial or resolution V fractional factorial design with axial points can produce this design [36].

For those situations in which the limits specified for factor settings are truly limits, the central composite inscribed (CCI) design uses the factor settings as the axial points and creates a factorial or fractional factorial design within those limits (in other words, a CCI design is a scaled down CCC design with each factor level of the CCC design divided by α to generate the CCI design) [36]. This design also requires 5 levels of each factor.

The other special design is called the face centered cube (CCF) design. In this design the axial points are at the center of each face of the factorial space, so $\alpha = \pm 1$. If the diamond points move to the face in the cube, then the design is CCF. This variety requires

3 levels of each factor. Augmenting an existing factorial or resolution V design with appropriate axial points can also produce this design.

The diagrams in Fig. 2.3 illustrate the three types of central composite designs for two factors. Note that the CCC explores the largest process space and the CCI explores the smallest process space. Both the CCC and CCI are rotatable designs, but the CCF is not. In the CCC design, the design points describe a circle circumscribed about the factorial square. For three factors, the CCC design points describe a sphere around the factorial cube. To maintain rotatability, the value of α depends on the number of experimental runs in the factorial portion of the central composite design:

$$\alpha = [n_c]^{1/4}, \quad (2.3)$$

where n_c is the number of experimental runs in the factorial portion of the central composite design. However, the factorial portion can also be a fractional factorial design of resolution V [36, 39].

2.3 Models Construction

It is necessary to develop an approximate model for the true response surface. If n observations are collected in an experiment, the model for them takes the form [38]:

$$y = X\beta + \varepsilon, \quad (2.4)$$

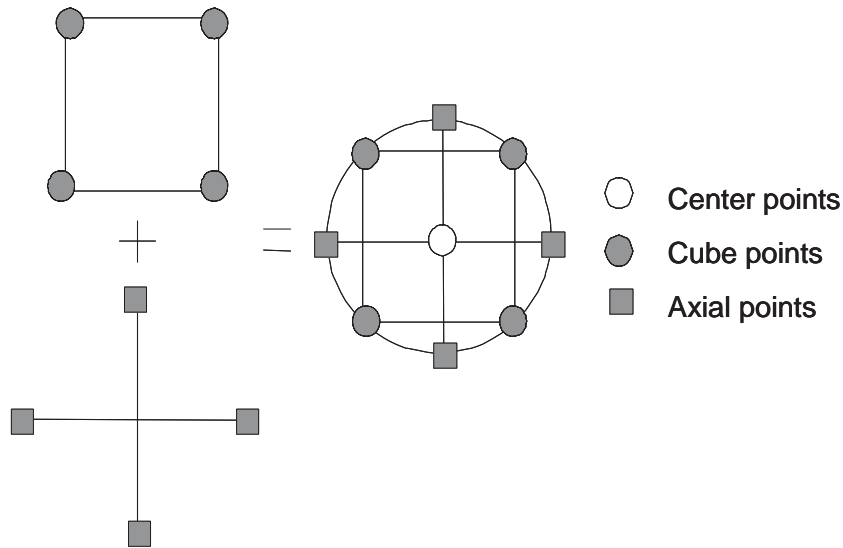


Figure 2.2: A central composite design of two factors. The design includes one center point, four cube points, and four axial points.

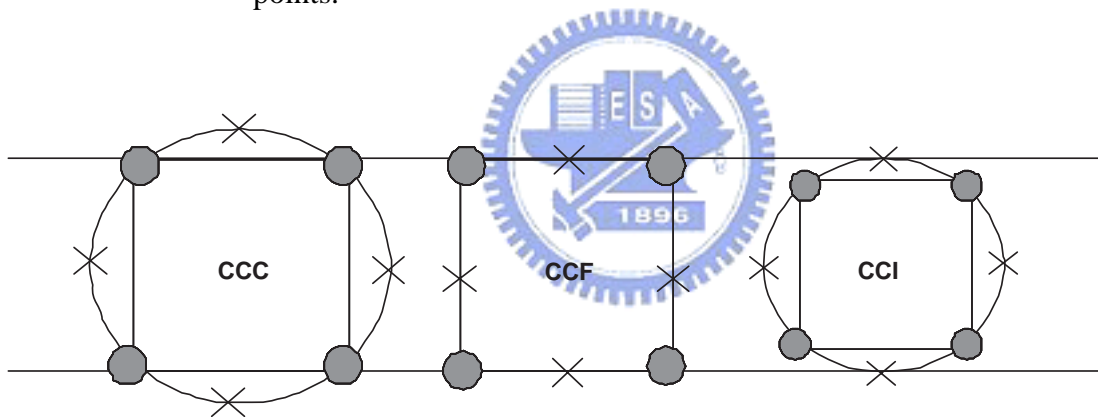


Figure 2.3: Comparison of the three types of central composite designs.

where

$$y = \begin{pmatrix} y_1 \\ y_2 \\ \vdots \\ y_n \end{pmatrix}, X = \begin{pmatrix} 1 & x_{11} & x_{12} & \cdots & x_{1k} \\ 1 & x_{21} & x_{22} & \cdots & x_{2k} \\ \vdots & \vdots & \vdots & & \vdots \\ 1 & x_{n1} & x_{n2} & \cdots & x_{nk} \end{pmatrix}, \beta = \begin{pmatrix} \beta_0 \\ \beta_1 \\ \vdots \\ \beta_k \end{pmatrix}, \varepsilon = \begin{pmatrix} \varepsilon_1 \\ \varepsilon_2 \\ \vdots \\ \varepsilon_n \end{pmatrix}.$$

In general, y is an $n \times 1$ vector of the observations, X is an $n \times p$ matrix of the levels of the independent variables, β is a $p \times 1$ vector of the regression coefficients, and ε is an $n \times 1$ vector of random errors.

We want to find the least squares estimators, $\hat{\beta}$, that minimizes

$$L = \sum_{i=1}^n \varepsilon_i^2 = \varepsilon^T \varepsilon = (y - X\beta)^T (y - X\beta). \quad (2.5)$$

As the result of our calculation, the least squares estimator of β is

$$\hat{\beta} = (X^T X)^{-1} X^T y. \quad (2.6)$$

The fitted regression model is

$$\hat{y} = X\hat{\beta}. \quad (2.7)$$

The difference between the responses y_i and the fitted value \hat{y}_i is a residual, say $e_i = y - \hat{y}$,

The vector of residual is denoted by:

$$\mathbf{e} = y - \hat{y}. \quad (2.8)$$

To check the normality assumption is by preparing a normal probability plot of the residual values. If the assumption holds, this plot will resemble a straight line. If the assumption is violated, a non-linear data transformation (e.g., $y' = \log(y)$) may be applied and new models are generated in an attempt to improve model adequacy [38]. A second plot showing the residual values versus the predicted response values is used to verify if the variance of

the original observation is constant. A random scattering of the residual values indicates that no correlation exists between the observed variance and the mean level of the response [39].

To develop an estimator of this parameter consider the sum of squares of the residuals, say

$$SS_E = \sum_{i=1}^n (y_i - \hat{y}_i)^2 = \sum_{i=1}^n e_i^2 = e^T e. \quad (2.9)$$

Equation (2.9) is called the **error** or **residual of squares**, and it has $n - p$ degrees of freedom associated with it. It can be shown that

$$E(SS_E) = \sigma^2(n - p), \quad (2.10)$$

so an unbiased estimator of σ^2 is given by

$$\hat{\sigma}^2 = \frac{SS_E}{n - p}. \quad (2.11)$$

To determine if there is a linear relationship between the response variable y and a subset of the regressor variables x_1, x_2, \dots, x_k is the test for significance of regression. The appropriate hypotheses are [38]:

$$\begin{aligned} H_0 & : \beta_1 = \beta_2 = \dots = \beta_k = 0, \\ H_1 & : \beta_j \neq 0 \text{ for at least one } j. \end{aligned} \quad (2.12)$$

If we reject H_0 , it implies that at least one of the regressor variables x_1, x_2, \dots, x_k contributes significantly to the model. The test procedure involves partitioning the total sum of

squares due to residual, say

$$SS_T = SS_R + SS_E. \quad (2.13)$$

A relatively simple procedure is performed to check for model significance in relation to random error. This test involves calculating the test statistic:

$$F_0 = \frac{MS_R}{MS_E} = \frac{SS_R/k}{SS_E/(n-k-1)} = \frac{\frac{1}{k} \sum_{j=1}^n (\hat{y}_i - \bar{y})^2}{\frac{1}{n-k-1} \sum_{j=1}^n (y_i - \hat{y}_i)^2}, \quad (2.14)$$

where \bar{y} is the average of measured response values. y_i , \hat{y}_i , and n are the i th measured response, the i th predicted response, and the number of simulated runs, respectively [38].

If this statistic exceeds the corresponding value of the F distribution value ($F_{\alpha,k,n-k-1}$), the response model is considered significant in relation to random error.

A second statistic, the coefficient of multiple determination R^2 is defined as:

$$R^2 = \frac{SS_R}{SS_T} = 1 - \frac{SS_E}{SS_T} = 1 - \frac{\sum_{i=1}^n (y_i - \hat{y}_i)^2}{\sum_{i=1}^n (y_i - \bar{y})^2}. \quad (2.15)$$

R^2 measures the amount of reduction in variability of the response y achieved, using the input factors x_1, x_2, \dots, x_k . From Eq. (2.13) we see that R^2 varies from zero to one [38][39]. However, a large value of R^2 does not necessarily imply that the regression model is good one. Adding a variable to the model will always increase R^2 , regardless of whether the additional variable is statistically significant or not. About this problem, some regression model builders prefer to use an adjusted R^2 statistic defined as

$$R_{adj}^2 = 1 - \frac{SS_E/(n-k-1)}{SS_T/(n-1)} = 1 - \frac{n-1}{n-k-1} (1 - R^2). \quad (2.16)$$

In general, the adjusted R^2 statistic will not always increase as variables are added to the model. In fact, if unnecessary terms are added, the value of R_{adj}^2 will often decrease.

2.4 Variable Selection

In response surface work it is customary to construct the full model corresponding to the situation at hand. That is, in steepest ascent we usually build the full first-order model, and in the analysis of a second-order model we usually construct the full quadratic. An experimenter may encounter situations where the full model may not be appropriate; that is, a model based on a subset of the regressors in the full model may be superior. Variable selection or model-building techniques may be used to identify the best subset of regressors to include in a regression model [39].

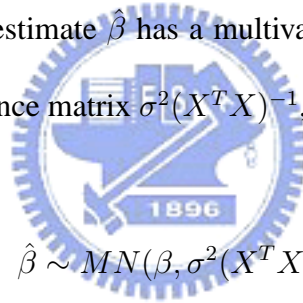
Variable selection is determined by statistical analysis of the generated response surface models. Input factors showing a significant effect on an individual response can be systematically determined using statistical techniques. Variations of these significant input factors will produce the greatest fluctuations in device performance. This analysis is extremely useful in understanding what areas of manufacturing require greater control.

(1) Half-normal plot and t test

As screening design, a technique for identifying significant model terms can be based

on the half-normal plot of model coefficients. This method is originally proposed for analyzing two-level factorial experiments applicable in cases where no degrees of freedom are available for estimating the variance of an error term. The effects are plotted on half-normal probability paper, those standing apart being identified as potentially real effects [40]. Probability plotting may also be used for experiments having three level. One approach is to express the effects with linear and quadratic components, and construct the normal probability plot of those components standardized to have the same variance [41][42].

The half-normal plots are informal graphical methods involving visual judgment. A formal test of effect significance is called t test for the least squares estimate $\hat{\beta}$. It can be shown that the least squares estimate $\hat{\beta}$ has a multivariate normal distribution with mean vector β and variance-covariance matrix $\sigma^2(X^T X)^{-1}$, i.e.,



$$\hat{\beta} \sim MN(\beta, \sigma^2(X^T X)^{-1}), \quad (2.17)$$

where MN stands for multivariate normal. The (i, j) th entry of the variance-covariance matrix is $Cov(\hat{\beta}_i, \hat{\beta}_j)$ and the j th diagonal element is $Cov(\hat{\beta}_j, \hat{\beta}_j) = Var(\hat{\beta}_j)$. Therefore, the distribution for the individual $\hat{\beta}_j$ is $N(\beta_j, \sigma_{jj}^2(X^T X)^{-1})$, which suggests that for testing the null hypothesis

$$H_0 : \beta_j = 0, \quad (2.18)$$

the following t statistic be used:

$$\frac{\hat{\beta}_j}{\sqrt{\hat{\sigma}_{jj}^2(X^T X)^{-1}}} \sim t_{N-p-1} \quad (\text{under } H_0). \quad (2.19)$$

Under H_0 , it has a t distribution with $N - p - 1$ degrees of freedom.

(2) Stepwise regression

Alternative of variable selection is called *stepwise regression*. It is one of various methods for evaluating only a small number of subset regression models by either adding or deleting regressors one at a time. Stepwise regression is a popular combination of procedures forward selection and backward elimination [38].

The procedure of the forward selection begins with the assumption that there are no regressors in the model other than the intercept. An effort is made to find an optimal subset by inserting regressors into the model one at a time. The first regressor selected for entry into the equation is the one that has the largest simple correlation with the response variable y . Suppose that this regressor is x_1 . This is also the regressor that will produce the largest value of the F-statistic for testing significance of regression. This regressor is entered if the F-statistic exceeds a preselected F-value, say F_{IN} (or F-to-enter). The second regressor chosen for entry is the one that now has the largest correlation with y after adjusting for the effect of the first regressor entered (x_1) on y . We refer to these correlations as partial correlations. They are the simple correlations between the residuals from the regression $\hat{y} = \hat{\beta}_0 + \hat{\beta}_1 x_1$ and the residuals from the regressions of the other candidate regressors on

x_1 , say $\hat{x}_j = \hat{\alpha}_{0j} + \hat{\alpha}_{1j}x_1$, $j = 2, 3, \dots, K$.

Suppose that at Step 2 the regressor with the highest partial correlation with y is x_2 .

This implies that the largest partial F-statistic is

$$F = \frac{SS_R(x_2|x_1)}{MS_E(x_1, x_2)}. \quad (2.20)$$

If this F-value exceeds F_{IN} , then x_2 is added to the model. In general, at each step the regressor having the highest partial correlation with y (or equivalently the largest partial F-statistic given the other regressors already in the model) is added to the model if its partial F-statistic exceeds the preselected entry level F_{IN} [38]. The procedure terminates either when the partial F-statistic at a particular step does not exceed F_{IN} or when the last candidate regressor is added to the model.

Forward selection begins with no regressors in the model and attempts to insert variables until a suitable model is obtained. Backward elimination attempts to find a good model by working in the opposite direction. That is, we begin with a model that includes all K candidate regressors. Then the partial F-statistic (or a t -statistic, which is equivalent) is computed for each regressor as if it is the last variable to enter the model. The smallest of these partial F-statistics is compared with a preselected value, F_{OUT} (or F-to-move); and if the smallest partial F-value is less than F_{OUT} , that regressor is removed from the model. Now a regression model with $K - 1$ regressors is constructed, the partial F-statistics for

this new model calculated, and the procedure repeated. The backward elimination algorithm terminates when the smallest partial F-value is not less than the preselected cutoff value F_{OUT} [38].

Backward elimination is often a very good variable selection procedure. It is particularly favored by analysts who like to see the effect of including all the candidate regressors, just so that nothing obvious will be missed. The two procedures described above suggest a number of possible combinations. One of the most popular is the stepwise regression algorithm and the flowchart is shown in Fig. 2.4 This is a modification of forward selection in which at each step all regressors entered into the model previously are reassessed via their partial F- or t -statistics. A regressor added at an earlier step may now be redundant because of the relationship between it and regressors now in the equation. If the partial F-statistic for a variable is less than F_{OUT} , that variable is dropped from the model.

Stepwise regression requires two cutoff values, F_{IN} and F_{OUT} . Several analysts prefer to choose $F_{IN} = F_{OUT}$, although this is not necessary. Sometimes we choose $F_{IN} > F_{OUT}$, making it more difficult to add a regressor than to delete one [38].

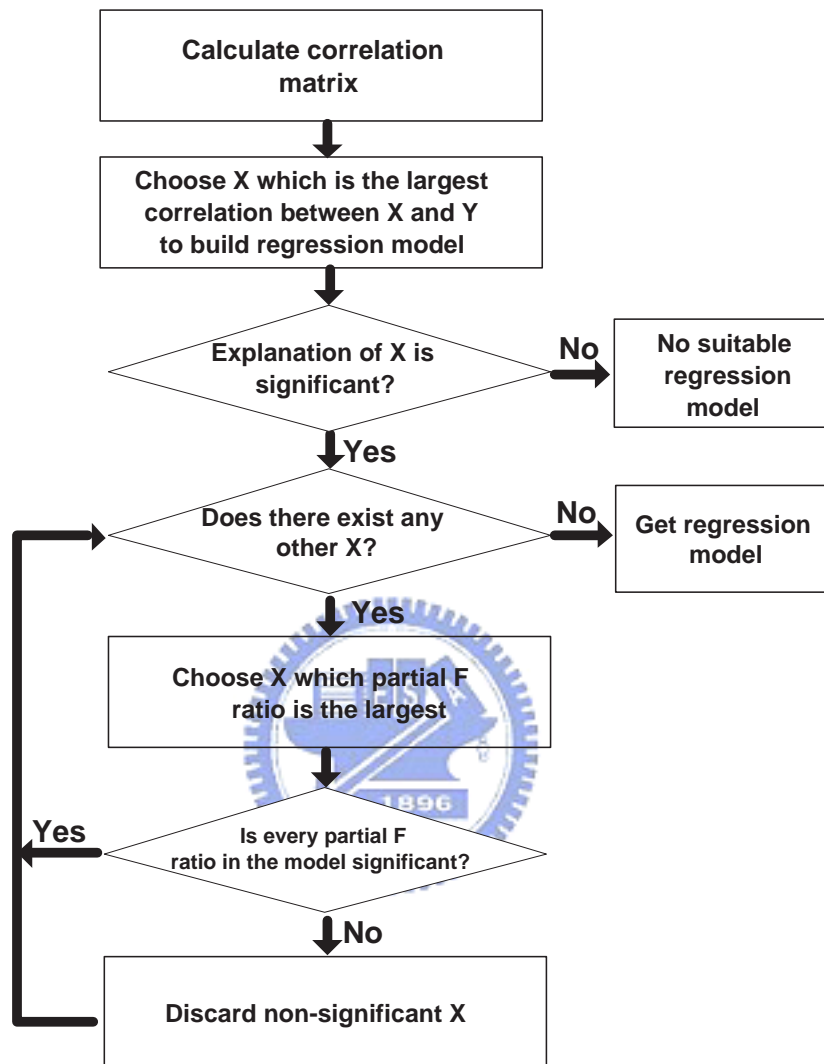


Figure 2.4: A flowchart of the stepwise regression algorithm used in our work.

2.5 Model Adequacy Checking

To checking the fitted model is an adequate approximation to the true system or not is always necessary. Also, we must verify that none of the least squares regression assumptions are violated. In this section we present several techniques for checking model adequacy [38].

(1) The normality assumption : The residuals are defined by Eq. (2.8), and they play an very important role in determining model adequacy. An useful method is to construct a normal probability plot of the residuals, as in Fig. 2.5. If the residual normal probability plot is approximately along a straight line, then the normality assumption of residuals is satisfied. When this plot indicates problems with the normality assumption, we often transform the response variable as a remedial measure [38][43]. Transformations are used for three purposes: stabilizing response variance, making the distribution of response variable closer to the normal distribution, and improving the fit of the model to the data.

We introduce transformation of the response variables called Box-Cox Method. The Box-Cox transformation is a particularly useful family of transformations. It is defined as:

$$y^\lambda = \begin{cases} \frac{y^{\lambda-1}}{\lambda}, & \lambda \neq 0 \\ \ln y, & \lambda = 0 \end{cases}, \quad (2.21)$$

where y is the response variable and λ is the transformation parameter. When λ is selected by the Box-Cox method, the experimenter can analyze the data using y^λ as the response,

unless of $\lambda = 0$, in which he can use $\ln y$. It is perfectly acceptable to use y^λ as the actual response, although the model parameter estimates will have a scale difference and origin shift in comparison to the results obtained using y^λ (or $\ln y$) [43].

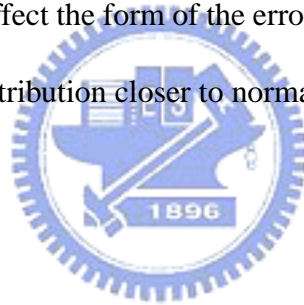
An approximate $100(1 - \alpha)$ percent confidence interval for λ can be found by calculating:

$$SS^* = SS_E(\lambda) \left(1 + \frac{t_{\alpha/2, \nu}^2}{\nu}\right), \quad (2.22)$$

where ν is the number of freedom. Plotting a graph of $SS_E(\lambda)$ versus λ , and then by locating the points on the λ axis where SS^* cuts the curve $SS_E(\lambda)$, we can read confidence limits on λ directly from the graph. If this confidence interval includes the value $\lambda = 1$, this implies that the datas do not support the need for transformation.

(2) Plot of residuals versus predicted value : If the model is correct and if the assumptions are satisfied, the residuals should be unrelated to any other variable including the predicted response. A simple check is to plot the residuals versus the predicted value \hat{y} . This plot should not reveal any obvious pattern, as in Fig. 2.6. A defect that occasionally shows up on this plot is nonconstant variance. Nonconstant variance also arises in cases where the data follow a nonnormal, skewed distribution because in skewed distributions the variance tends to be a function of the mean.

Considerable research has been devoted to the selection of an appropriate transformation. If experimenters know the theoretical distribution of the observations, they may utilize this information in choosing a transformation. For example, if the observations follow the Poisson distribution, the square root transformation $y_{ij}^* = \sqrt{y_{ij}}$ or $y_{ij}^* = \sqrt{1 + y_{ij}}$ is appropriate. If the data follow the lognormal distribution, the logarithmic transformation $y_{ij}^* = \log y_{ij}$ is appropriate. When there is no obvious transformation, the experimenter usually empirically seeks a transformation that equalizes the variance regardless of the value of the mean. Another approach is to select a transformation that minimizes the interaction mean square, resulting in an experiment that is easier to interpret. Transformations made for inequality of variance also affect the form of the error distribution. In most cases, the transformation brings the error distribution closer to normal [43].



2.6 Desirability Function

The desirability function is a useful tool to solve multiple responses. It was proposed by Derringer and Suich (1980) [43]. The desirability function d_i varies over the range $0 \leq d_i \leq 1$, where the $d_i = 0$ is representing a completely undesirable of y_i and $d_i = 1$ is representing a completely desirable or target response value of y_i . After multiple response are transformed into individual desirabilities, the individual desirabilities are then

combined using geometric mean to maximize the overall desirability D :

$$D = (d_1 \times d_2 \times \dots \times d_m)^{1/m}, \quad (2.23)$$

where m is the number of responses [43]. By the equation, if any d_i is equal to zero, then the overall desirability is zero.

According to the specification for the responses, response is to be maximized, minimized, or achieved a target value. For the i th response y_i is a maximum value,

$$d_i = \begin{cases} 0, & \hat{y}_i < L_i \\ \left(\frac{\hat{y}_i - L_i}{T_i - L_i}\right)^s, & L_i \leq \hat{y}_i \leq T_i \\ 1, & \hat{y}_i > T_i \end{cases} \quad (2.24)$$

For the response y_i is a minimum value,

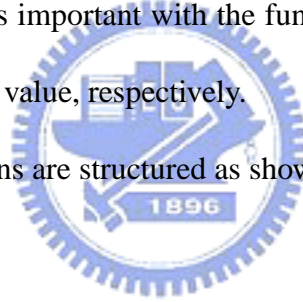
$$d_i = \begin{cases} 1, & \hat{y}_i < T_i \\ \left(\frac{U_i - \hat{y}_i}{U_i - T_i}\right)^s, & T_i \leq \hat{y}_i \leq U_i \\ 0, & \hat{y}_i > U_i \end{cases} \quad (2.25)$$

For the response is achieved a target value,

$$d_i = \begin{cases} 0, & \hat{y}_i < L_i \\ \left(\frac{\hat{y}_i - L_i}{T_i - L_i}\right)^s, & L_i \leq \hat{y}_i \leq T_i \\ \left(\frac{U_i - \hat{y}_i}{U_i - T_i}\right)^t, & T_i \leq \hat{y}_i \leq U_i \\ 0, & \hat{y}_i > U_i \end{cases}, \quad (2.26)$$

where the weight s and t determine how important it is close to the target value. When the weight $s = 1, t = 1$ the desirability function is liner. Choosing $s > 1, t > 1$ means more important to be close the target value with the function that is concave, and choosing $0 < s < 1, 0 < t < 1$ means this less important with the function that is convex. L_i, U_i , and T_i are the lower, upper, and target value, respectively.

The individual desirability functions are structured as shown in Fig. 2.7.



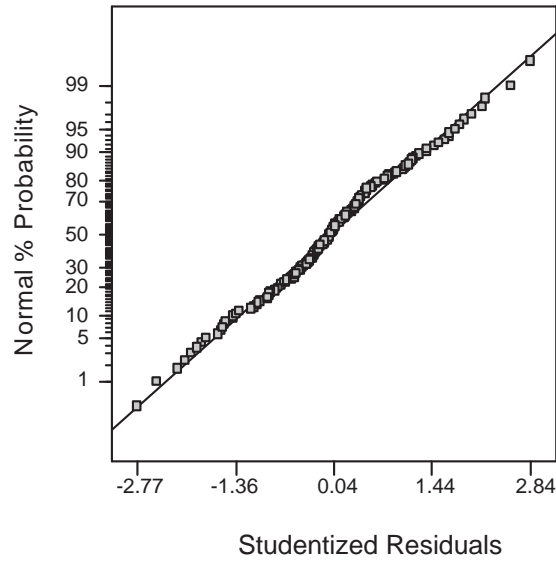


Figure 2.5: An example of residual normal probability plot. If the residual is close to the line, it will satisfy normality assumption. The studentized residuals are the standardized residuals adjusted for the distance from the average X value.

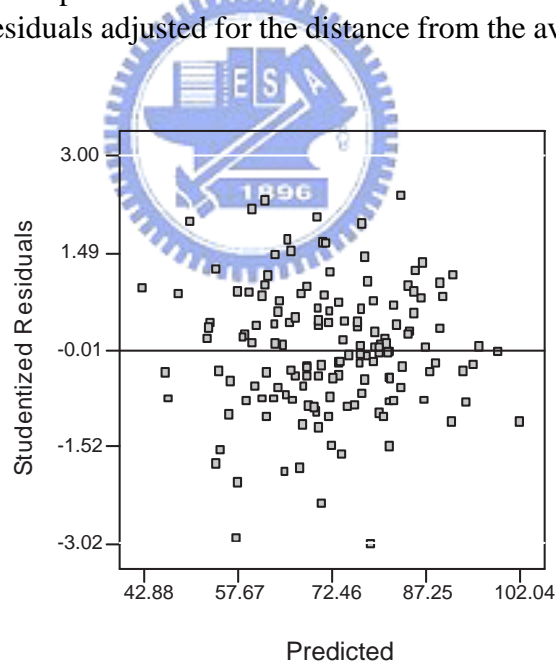


Figure 2.6: An example of scatter plot of predicted values versus residuals. This plot should not reveal to any obvious patterns. The studentized residuals are the standardized residuals adjusted for the distance from the average X value.

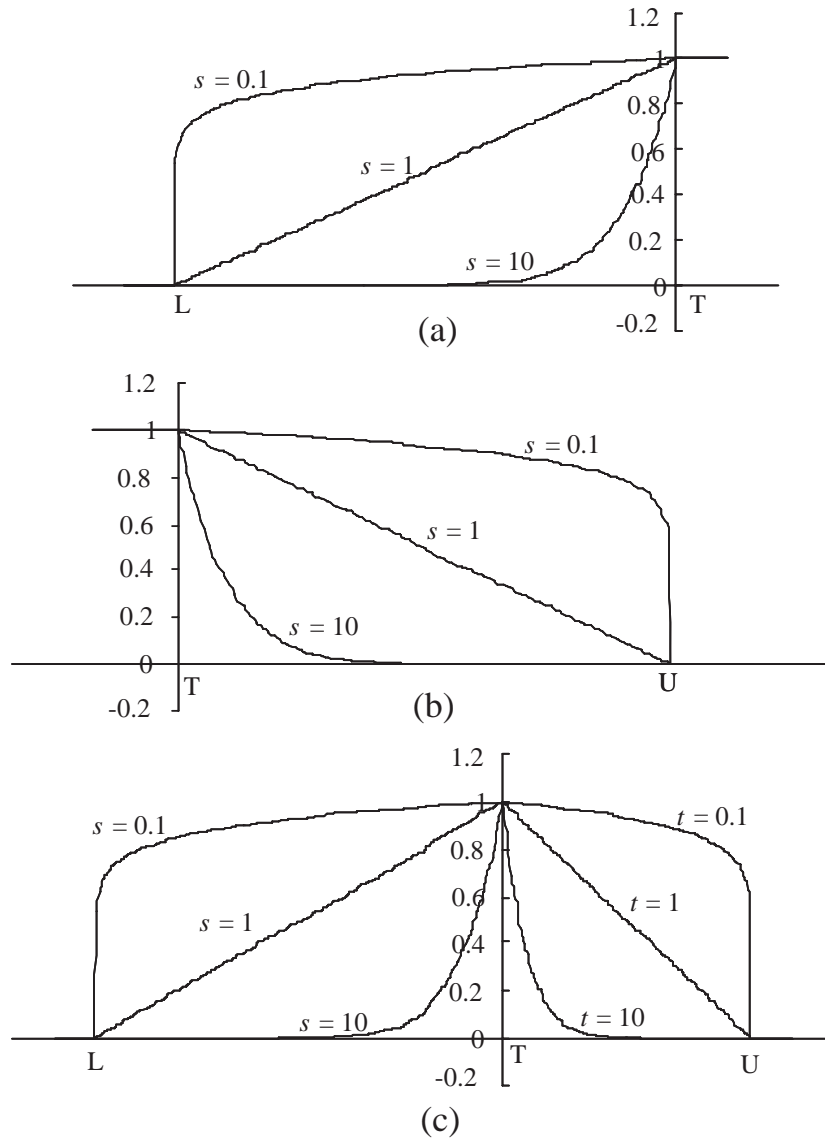


Figure 2.7: Individual desirability functions for the simultaneous optimization (a) objective is to maximize response, (b) objective is to minimize response, and (c) objective is for response which is assumed to be as close as possible to the target. The weights s and t determine how important it is close to the target value, and L , U , T are the lower, upper, and target value, respectively.

2.7 Other Design Methods

There are different types of design of experiment that have been widely applied to other designs such as Taguchi method and mixture design. We briefly describe their validation.

2.7.1 Taguchi Method

Many of the DOE concepts were popularized by Taguchi's contributions to the methodology of off-line quality design. The basis for his approach is to minimizing the loss to society that occurs when a products performance varies from a customer-specified target [44][45]. Taguchi's ideas for parameter and tolerance design have evolved into what industry labels Design of Experiments for robust product design. Taguchi introduced the DOE techniques to engineering for quality improvement. In the past, enhancements to the DOE technique have been used on a production line or laboratory to derive empirical models and optimize a given process. Some of the well-known Taguchi orthogonal arrays were given earlier when three-level, mixed-level and fractional factorial designs were discussed.

The aim of parameter design is to make a product or process less variable (more robust) in the face of variation over which we have little or no control. Taguchi advocated using inner and outer array designs to take into account noise factors (outer) and design factors (inner). We could have used fractional factorials for either the inner or outer array designs, or for both. The tolerance design of the design process concentrates on the selective

reduction of tolerances to reduce quality loss at the expense of increasing manufacturing costs.

2.7.2 Mixture Design

In a mixture experiment, the independent factors are proportions of different components of a blend. For example, if you want to optimize the tensile strength of stainless steel, the factors of interest should be the proportions of iron, copper, nickel, and chromium in the alloy. The fact that the proportions of the different factors must sum to 100 % complicates the design as well as the analysis of mixture experiments.

In mixture problems, the purpose of an experiment is to model the blending surface with some form of mathematical equation so that: (1) predictions of the response for any mixture or combination of the ingredients can be made empirically; (2) and some measure of the influence on the response of each component singly and in combination with other components can be obtained [36].

2.7.3 Comparison with the Popular Designs

DOE using Taguchi approach has become a much more attractive tool to practicing engineers and scientists. The objective of Taguchi approach is to obtain reproducible results and

Table 2.1: Difference between Taguchi approach and classical DOE.

Taguchi approach	Classical DOE
Standard approach	Methods are not standardized
Smaller number of experiments	Larger number of experiments
Standard method of noise factor	No standardized method of noise treatment
Seeks to find stable condition	Develops models
Used to solve engineering problems	Used to solve scientific experiments

robust products. The objective of classical DOE is to gather scientific knowledge about factor effects and their interactions. Difference between Taguchi approach and classical DOE is shown in Tab. 2.1 [46]. In this thesis, it is suitable for us to use the classical DOE to investigate the problem due to our data type.



2.8 Summary

In this chapter, we introduce the statistical methodology which is used in this work. Screening design is the first step in this work to select the significant factors. After this step, we have three type central composite design and choose one type among them to construct the response surface model. The basic of the response surface model and adequacy checking are then introduced. Then we discuss desirability function which is used to solve the multiple responses and according to this index we can optimize successfully. Finally we compare the difference between Taguchi approach and classical DOE, and we note that the

classical DOE is suitable for this work.



Chapter 3

Low Noise Amplifier

In this chapter, we discuss the low noise amplifier (LNA) circuit which will be one of our testing examples. Due to a large number of circuit simulations, it is necessary to produce the response data, where Hspice simulator is integrated in our method. This chapter is organized as follows: Section 3.1 describes characteristics of LNA circuit. Section 3.2 describes what problem we will discuss and Sec. 3.3 presents the usage of the circuit simulation. Finally, a summary of this chapter is given.

3.1 A LNA Circuit with Deep Submicron MOSFETs

LNA circuit is important to modern communication systems. The main object of LNA is to ensure the quality of signal in the process of receiving the signal. A LNA design presents

a considerable challenge because of its simultaneous requirement for high gain, low noise figure, good input and output matching and unconditional stability at the lowest possible current draw from the amplifier. In this experiment, the working frequency of the tested LNA circuit is from 2.11 to 2.17 GHz, shown in Fig. 3.1. The cascade low noise amplifier is constructed two transistor placed cascaded. Lload and Rload are the compact models of on-chip spiral inductors needed in our LNA circuit. The choke inductor Lchoke working at high frequency is fixed at 1 uH. Cin is an external signal couple capacitor is also fixed at 20 pF.



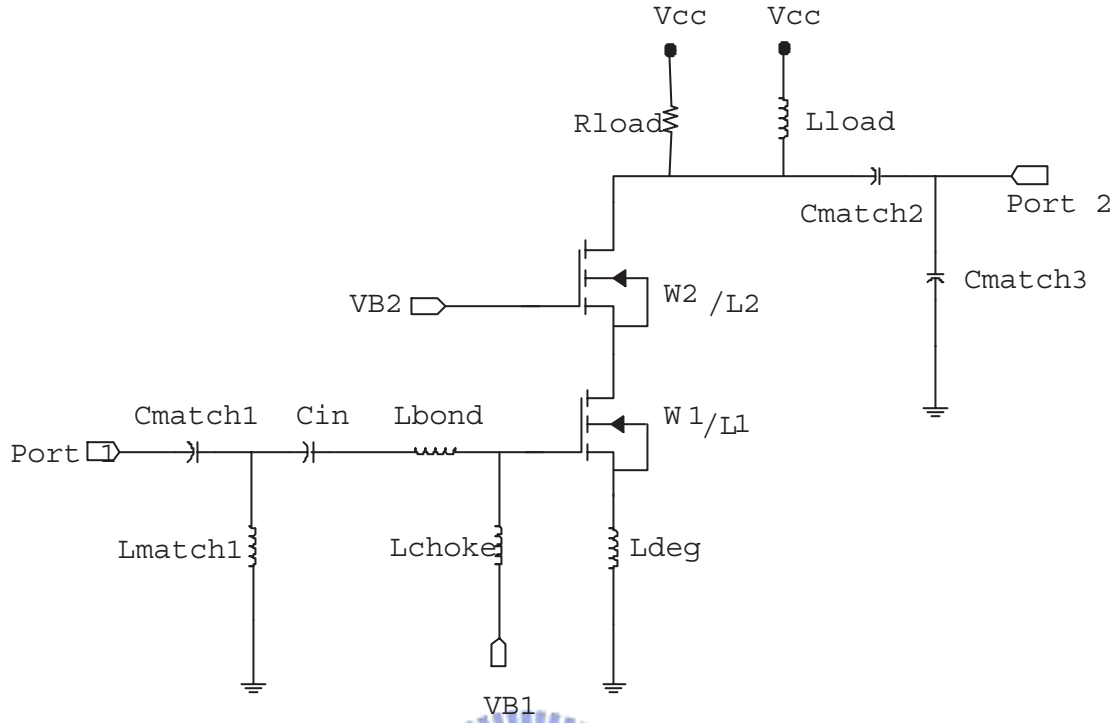


Figure 3.1: The explored LNA circuit in our experiment.

3.1.1 Noise Figure

The parameters we used to diagnose the noise of LNA are noise factor (F) and noise figure (NF). The noise factor of a low-noise amplifier is defined as the signal-to-noise ratio at the input divided by the signal-to-noise ratio at the output. The equation for noise factor and noise figure is given by

$$F = \frac{SNR_{in}}{SNR_{out}} = \frac{\frac{signal_{in}}{Noise_{in}}}{\frac{signal_{out}}{Noise_{out}}} = \frac{Noise_{in} + Noise_{amp}}{Noise_{in}} = 1 + \frac{Noise_{amp}}{Noise_{in}}, \quad (3.1)$$

$$NF = 10\log(F), \quad (3.2)$$

where SNR_{in} is the signal-to-noise ratio at the input and SNR_{out} is the signal-to-noise ratio at the output. $Noise_{in}$ is the noise from the previous stage, $Noise_{out}$ is the noise at the output which is additional noise from amplifier ($Noise_{amp}$) added the noise from $Noise_{in}$. Besides, in Eq. (3.1), $Noise_{amp}$ is always not zero, therefore, $F > 1$ and $NF > 0$ dB is consequential. In other words, SNR_{in} must be greater than SNR_{out} .

In a cascade amplifier the final stage has an input signal that consists of the original signal and noise amplified by each successive stage. Each stage in the cascade chain amplifies signals and noise from previous stages and contributes some noise of its own. The overall noise factor for a cascade amplifier is:



$$F = 1 + (F_1 - 1) + \frac{(F_2 - 1)}{A_{p1}} + \frac{(F_3 - 1)}{A_{p1}A_{p2}} + \dots$$

$$F_n = F_1 + \frac{(F_2 - 1)}{A_{p1}} + \dots + \frac{(F_n - 1)}{\prod_{i=1}^{n-1} A_{pi}}, \quad (3.3)$$

where F is the overall noise factor in cascade, F_i is the noise factor of the i th stage, A_{pi} is the gain of the i th stage. F_n is the overall noise factor of n stages in cascade. As show in Eq. (3.3), the noise factor of the entire cascade chain is determined by the the first stage noise factor because the noise factors of the second and subsequent stages are divided by

the previous stage gains when referred back to the input. High gain and low noise low-noise amplifiers typically use a low-noise amplifier circuit for only the first stage or two in the cascade chain to achieve an overall noise factor.

3.1.2 Stability Factor

Unconditional stability of the circuit is the target of the LNA designer. It is a critical concern in designing a low noise amplifier. The stability of circuit can be determined by S-parameter of transistors, and the matching network of every stage. S-parameters provided by the manufacturer of the transistor will aid in stability analysis of the LNA circuit. Two main methods exist in S-parameter stability analysis: numerical and graphical. Numerical analysis consists of calculating a term called Rollett Stability Factor K [11][12][13]. An intermitted quantity called delta (Δ) should be calculated first to simplify the final equation for the K-factor.

$$\Delta = S_{11} * S_{22} - S_{21} * S_{12}, \quad (3.4)$$

then

$$K = \frac{1 + |\Delta|^2 - |S_{11}|^2 - |S_{12}|^2}{2 * |S_{11}| * |S_{12}|}. \quad (3.5)$$

When the K factor is greater than unity, the circuit will be unconditionally stable for any combination of source and load impedance. When K is less than unity, the circuit is potentially unstable and oscillation may occur with a certain combination of source and/or load

impedance presented to the transistor. The K factor represents a quick check for stability at given frequency and given bias condition. A sweep of the K-factor over frequency for a given biasing point should be performed to ensure unconditional stability outside of the band of operation.

3.2 Linearity

There are two different limitations in determining the dynamic range of the amplifier (Fig. 3.2), one is noise and the other is linearity. Usually, noise figure sets the limitation on minimum signal strength, and linearity limits the maximum signal strength. Hence, linearity is equally as important as noise figure in the design of a low noise amplifier. In the case of base band amplifiers, total harmonic distortion is usually used to represent their linearity. On the other hand, RF amplifiers often use IIP3, IIP2, or the 1 dB gain compression point to represent their linearity. The IIP3 of each stage must sufficiently high to reduce nonlinearity.

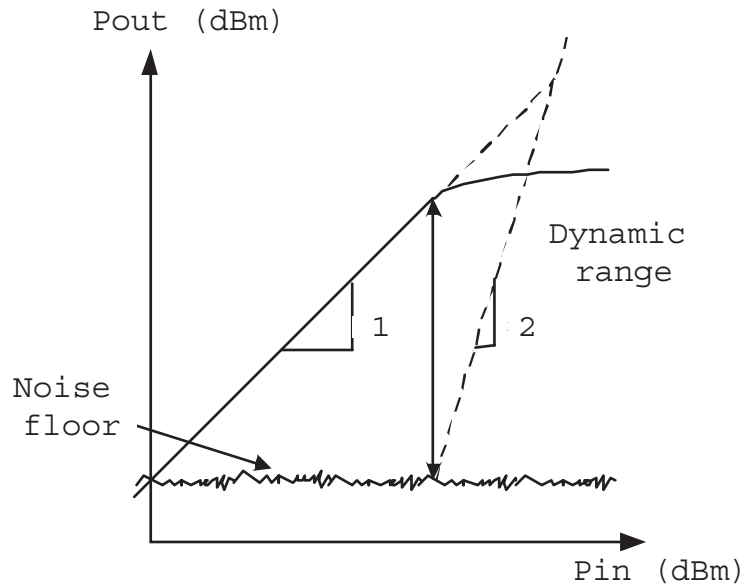


Figure 3.2: An illustration of spurious-free dynamic range with the noise floor and IIP3.

3.3 Problem Description

In the integrated circuit design, people consider efficiency, reliability and stability. Furthermore, there are also some constrains for the electrical and physical characteristics. In our work, we are interested in seven physical characteristics with specific performance, and they are:

- (1) $S_{11} < -10\text{dB}$ at working region;
- (2) $S_{12} < -25\text{dB}$ at working region;
- (3) S_{21} parameter is as great as possible at working region;
- (4) $S_{22} < -10\text{dB}$ at working region;

- (5) K factor > 1 at working region;
- (6) NF < 2 dB at working region;
- (7) IIP3 > -10 dB.

The working region is from 2.11 GHz to 2.17 GHz. The goal of our optimization problem is to adjust some parameters, such as capacitance, inductance and resistance, to achieve the requirements of each characteristic.

3.4 Circuit Simulators

In this work, the SPICE is considered as a circuit simulation tool. After designing a proper experiment, we will get the response data from SPICE. To perform circuit simulation, a set of model parameter and the designed circuit file are requested. The circuit simulator simulate the circuit and output the required characteristics noted in circuit file. The execution flow is shown in Fig. 3.3 and the netlist of this LNA circuit is shown in Appendix B.

Although gain, noise figure, stability, linearity and input and output match are all equally important, they are dependent and do not always work in each other's favor. Most of these conditions can be met by carefully selecting a transistor and understanding parameter trade-offs. The RF compact spice netlist that we apply is shown in Appendix B and the equivalent circuit is presented in Fig. 3.4.

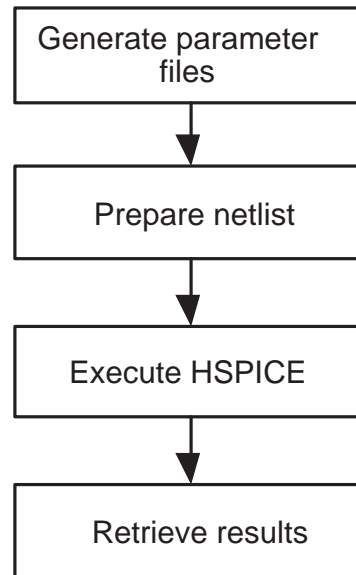



Figure 3.3: A flow of circuit simulation.

3.5 Summary



A LNA circuit composed with $0.25 \mu\text{m}$ metal-oxide-silicon field effect transistors (MOS-FETs) is discussed as the applied example. In this chapter the target LNA circuit is introduced and the method that adopts the circuit simulator is described. We will study the relationship between the circuit performance and its circuit parameters. Circuit performance that we are interested consist of input return loss, output return loss, reverse isolation, voltage gain, k factor, noise figure, and input third-order intercept point.

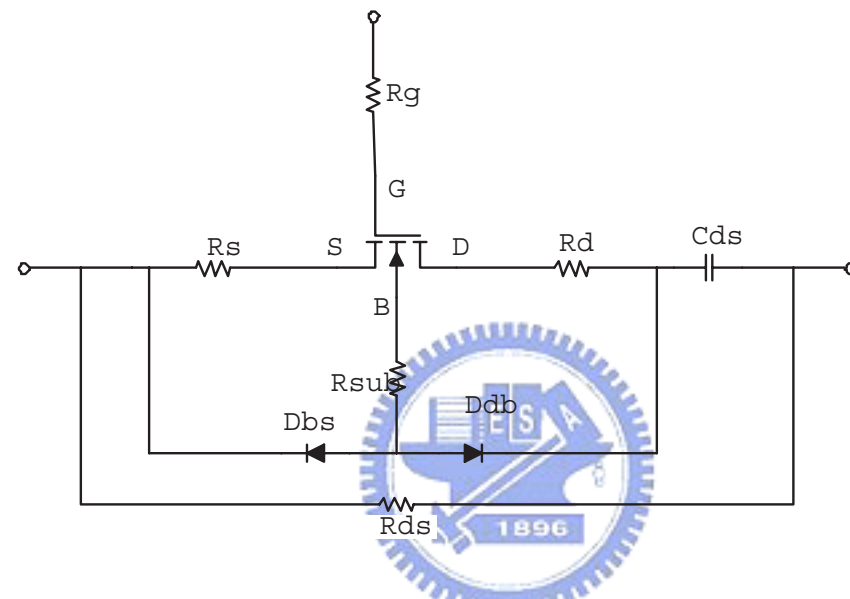


Figure 3.4: A RF model applied in this work.

Chapter 4

Results of DOE for LNA Circuit



4.1 Results of The Screening Design

First, we denote the Rload and Lload as **Load**, and they have the same value. The levels of screening design for each factors are provided in Tab. 4.1. The fractional factorial design with resolution IV is used.

4.1.1 The Fractional Factorial Design

A 2_{IV}^{13-8} fractional factorial design with resolution IV is used in the screening design, and the generators used are:

$$\begin{aligned}
 F &= A \times B \times C & G &= A \times B \times D \\
 H &= A \times C \times D & J &= B \times C \times D \\
 K &= A \times B \times E & L &= A \times C \times E \\
 M &= A \times D \times E & N &= B \times C \times E,
 \end{aligned} \tag{4.1}$$

where A is Cmatch1, B is Cmatch2, C is Cmatch3, D is Ldeg, E is Lmatch1, F is L1, g is W1, H is VB1, J is VB2, and K is VDD.

Before performing an experiment for the fractional factorial design with resolution IV, we fix the Load factor because the value of Load is discrete and is difficult for discussion. We fix the Load factor at 4.5, and the voltage gain very close to our target. Table 4.3 presents the minimum and maximum of seven responses in the different settings of Load factor. Clearly, we determine the value of Load at 4.5 is helpful for this work. So there are 13 factors in the screening design. In the screening design, some factors are varied by $\pm 10\%$ about their nominal value; and due to restriction, some factors are varied by more smaller range, for example, the difference between VB2 and VDD is less than 0.25V. They are varied by $\pm 4.5\%$. The levels of the screening design for each factor are shown in Tab. 4.1.

After the experiment for the fractional factorial design with resolution IV for 13 factors, 7 half-normal plots are drawn to select the significant factors. The half-normal plots of these 7 responses are shown in Figs. 4.1-4.7, and the result is shown in Tab. 4.2. In the table the numbers present the order of significant effect, and "1" means the most important to the corresponding response. We select the factor which uses the 'union' concept. And we only consider the main effects because main effects and three-factor interactions are aliases, three-factor interactions are neglected. Besides, two-factor interactions are aliased with each other. Therefore, because the only three main effects are eliminated, we don't consider any significant two-factor interactions. Finally, we remove three factors which are Lbond, L2, and W2.

4.1.2 Summary



In this section, 10 significant factors have successfully been selected from the screening design. They are **Cmatch1**, **Cmatch2**, **Cmatch3**, **Ldeg**, **Lmatch1**, **L1**, **W1**, **VB1**, **VB2**, and **VDD**. We use a 2_{IV}^{13-8} fractional factorial design to calculate 13 factor effects, and use half-normal plots to select the significant factors. The levels of screening design for 13 factors are shown in Tab. 4.1.

Table 4.1: The levels of screening design for the 13 factors.

	Center value	Cube
Factor name	0	± 1
A: Cmatch1 (F)	658	$\pm 10\%$
B: Cmatch2 (P)	1.7	$\pm 5\%$
C: Cmatch3 (P)	4.5	$\pm 5\%$
D: Lbond (N)	1	$\pm 10\%$
E: Ldeg (N)	1	$\pm 10\%$
F: Lmatch1 (N)	4.6	$\pm 10\%$
G: L1 (μm)	0.25	± 0.01
H: L2 (μm)	0.25	± 0.01
J: W1 (μm)	5	± 0.5
K: W2 (μm)	5	± 0.5
L: VB1 (V)	0.75	$\pm 10\%$
M: VB2 (V)	2.7	$\pm 4.5\%$
N: VDD (V)	2.7	$\pm 4.5\%$

Table 4.2: A list of the results for the screening design, where "1" means the most important term with respect to the corresponding response.

	S11	S12	S21	S22	K	NF	IIP3
A: Cmatch1	3	6	5			2	
B: Cmatch2		5	4	1			
C: Cmatch3		4	6	2			
D: Lbond							
E: Ldeg			3		2	4	4
F: Lmatch1	1	1	2			1	5
G: L1			8		3		
H: L2							
J: W1	2	2	7		4	3	
K: W2							
L: VB1		3	1		1	2	2
M: VB2							1
N: VDD					5		1

Table 4.3: The minimum and maximum of seven responses in the six settings of Load. The Load factor is 4.5 which makes the voltage gain close to our target.

		Load= 1.5		Load= 2.5	
response	goal	minimum	maximum	minimum	maximum
S11	< -10	-20.41	-2.417	-20.39	-2.402
S12	< -25	-67.25	-61.34	-61.05	-54.89
S21	maximized	-14.81	-9.19	-8.337	-2.8
S22	< -10	-0.051	-0.027	-0.156	-0.078
K	> 1	18.26	29.86	13.06	21.13
NF	< 2	1	2.67	0.916	2.437
IIP3	> -10	0.3	10.77	0.515	11.55
		Load= 3.5		Load= 4.5	
response	goal	minimum	maximum	minimum	maximum
S11	< -10	-20.41	-2.369	-21.92	-2.514
S12	< -25	-52.87	-46.12	-42.64	-37.83
S21	maximized	0.274	5.906	9.752	14.59
S22	< -10	-0.71	-0.30	-8.79	-3.49
K	> 1	8.21	12.92	5.841	8.93
NF	< 2	0.83	2.21	0.79	2.09
IIP3	> -10	0.995	10.505	-11.005	3.405
		Load= 5.5		Load= 6.5	
response	goal	minimum	maximum	minimum	maximum
S11	< -10	-25.13	-2.811	-22.26	-2.654
S12	< -25	-47.97	-41.14	-51.01	-45.23
S21	maximized	4.054	11.91	0.5667	8.042
S22	< -10	-1.421	-0.6178	-0.464	-0.2629
K	> 1	4.729	7.053	4.152	6.135
NF	< 2	0.770	2.033	0.761	2.006
IIP3	> -10	-5.46	5.63	-1.155	8.64

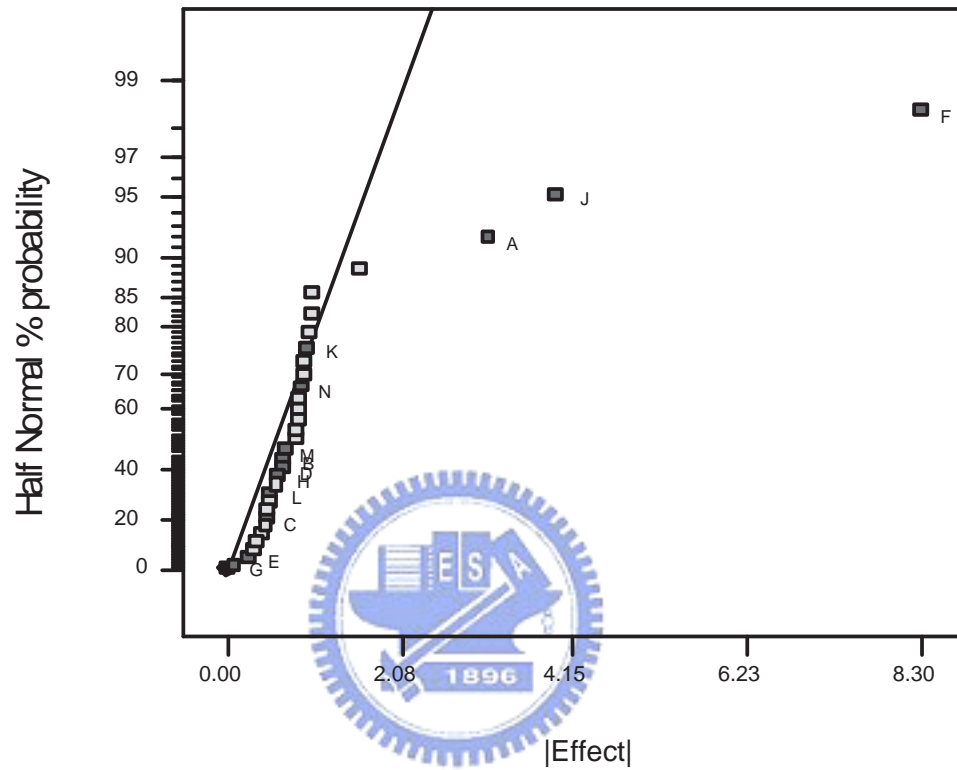


Figure 4.1: A half-normal plot for the effect of S11. The factors are (A) Cmatch1, (B) Cmatch2, (C) Cmatch3, (D) Ldeg, (E) Lmatch1, (F) L1, (g) W1, (H) VB1, (J) VB2, and (K) VDD.

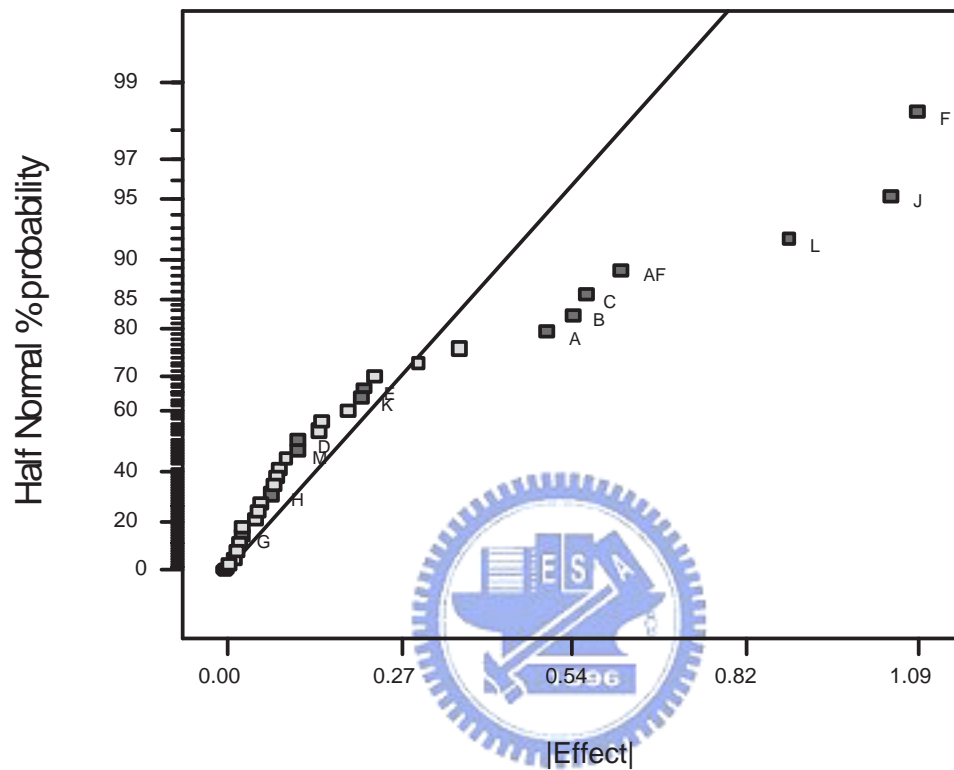


Figure 4.2: A half-normal plot for the effect of S12. The factors are (A) Cmatch1, (B) Cmatch2, (C) Cmatch3, (D) Ldeg, (E) Lmatch1, (F) L1, (g) W1, (H) VB1, (J) VB2, and (K) VDD.

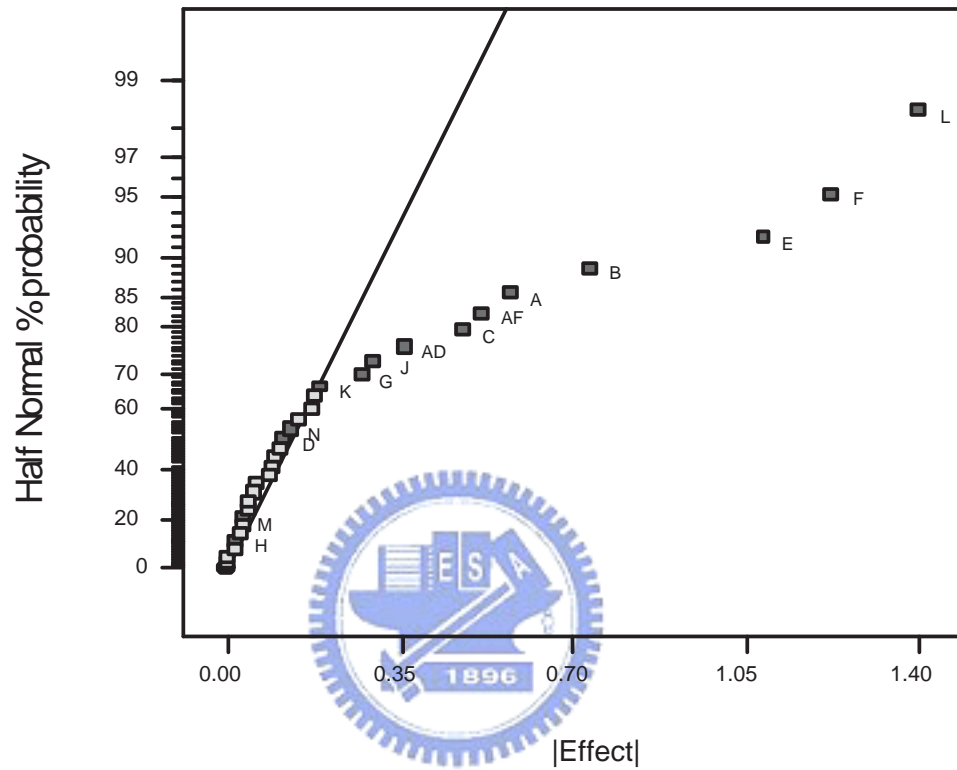


Figure 4.3: A half-normal plot for the effect of S21. The factors are (A) Cmatch1, (B) Cmatch2, (C) Cmatch3, (D) Ldeg, (E) Lmatch1, (F) L1, (g) W1, (H) VB1, (J) VB2, and (K) VDD.

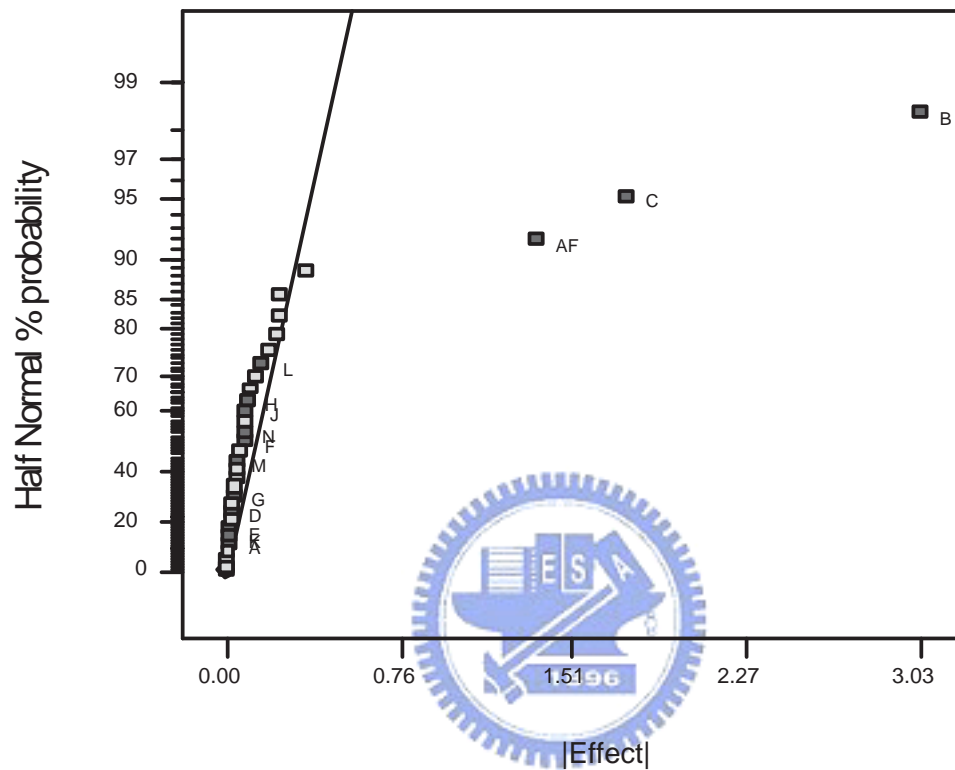


Figure 4.4: A half-normal plot for the effect of S22. The factors are (A) Cmatch1, (B) Cmatch2, (C) Cmatch3, (D) Ldeg, (E) Lmatch1, (F) L1, (g) W1, (H) VB1, (J) VB2, and (K) VDD.

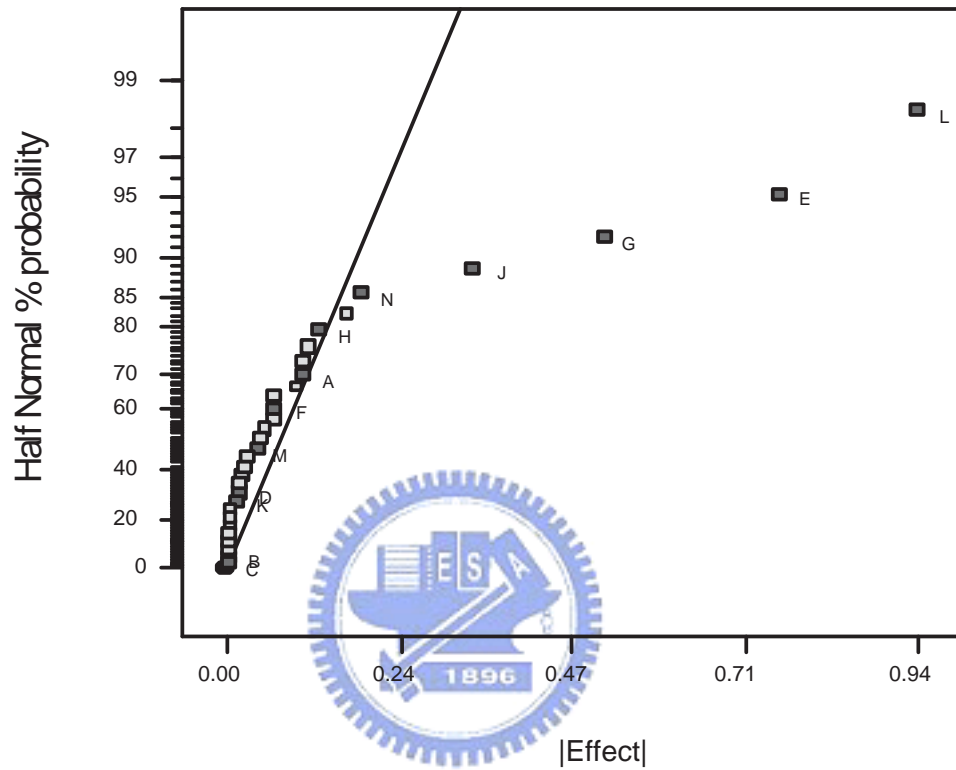


Figure 4.5: A half-normal plot for the effect of K. The factors are (A) Cmatch1, (B) Cmatch2, (C) Cmatch3, (D) Ldeg, (E) Lmatch1, (F) L1, (g) W1, (H) VB1, (J) VB2, and (K) VDD.

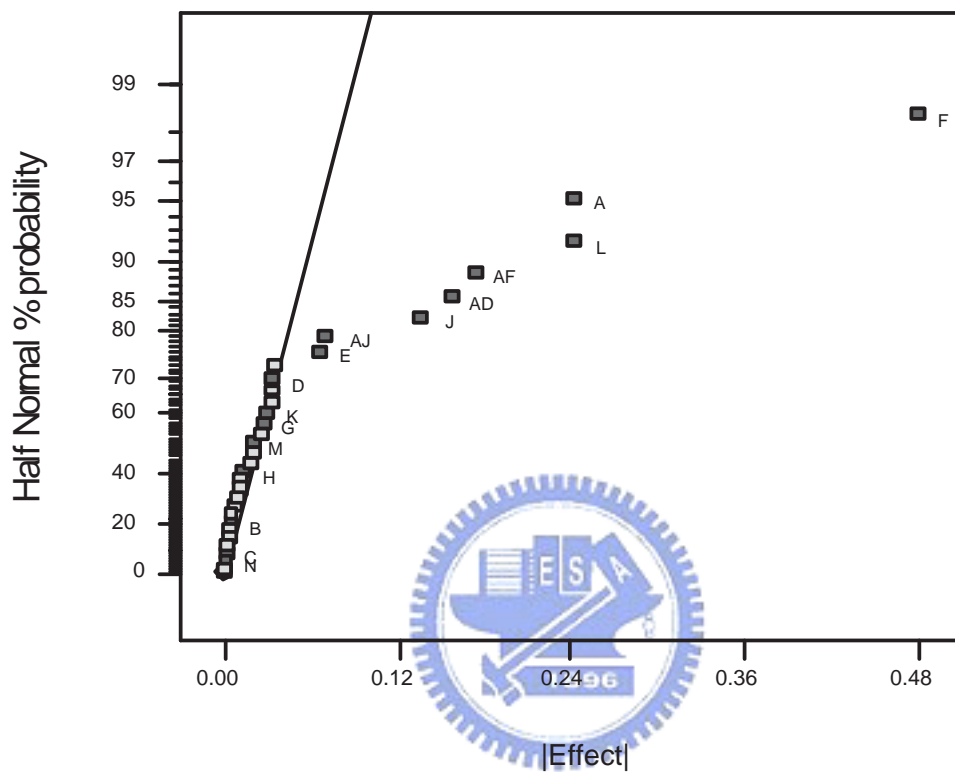


Figure 4.6: A half-normal plot for the effect of NF. The factors are (A) Cmatch1, (B) Cmatch2, (C) Cmatch3, (D) Ldeg, (E) Lmatch1, (F) L1, (g) W1, (H) VB1, (J) VB2, and (K) VDD.

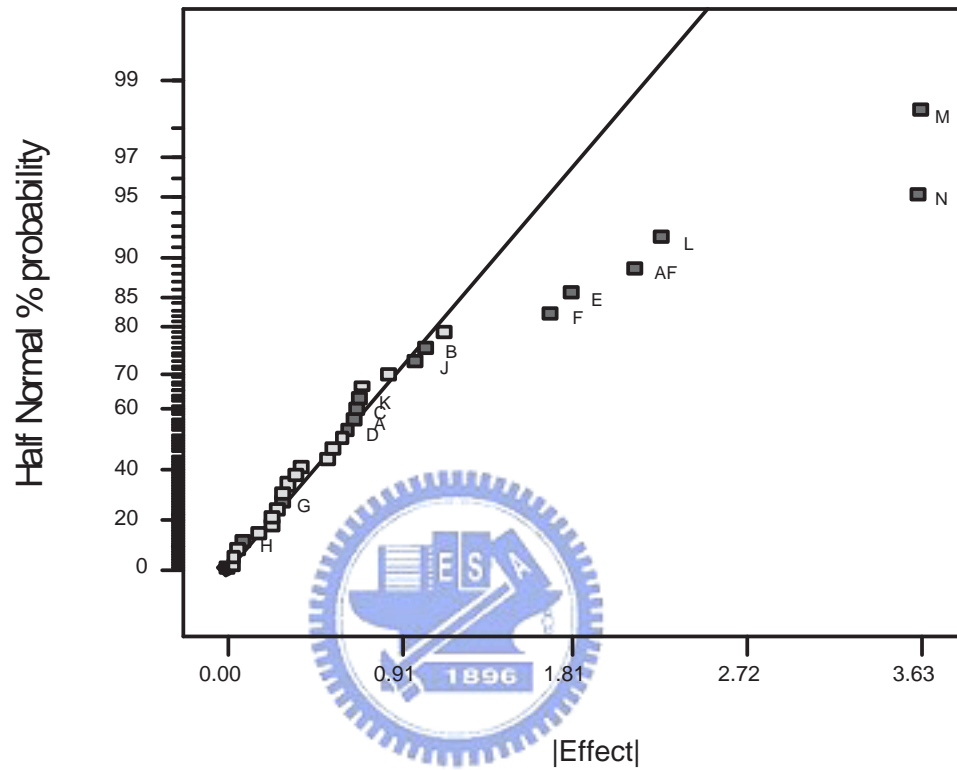


Figure 4.7: A half-normal plot for the effect of IIP3. The factors are (A) Cmatch1, (B) Cmatch2, (C) Cmatch3, (D) Ldeg, (E) Lmatch1, (F) L1, (g) W1, (H) VB1, (J) VB2, and (K) VDD.

4.2 Results of The Central Composite Design

In this chapter we discuss the results of the central composite design. From the screening design we have selected 10 factors for our next design, and the face centered cube design (CCF) is used.

4.2.1 The Face Centered Cube Design

To generate the necessary data for construction of the quadratic response models, 149 experimental runs are completed by calling HSPICE. We choose the CCF design from the three type of the CCD that we introduced in Chap. 2, because the CCF design is more suitable for designing the response surface models [39]. The levels of the first CCF design for 10 factors are the same with the screening design. From the CCF design, 1 center point, 20 axial points, and 2_V^{10-3} cube points which is fractional factorial design with resolution V are used, and the generators are:

$$VB1 = Cmatch1 \times Cmatch2 \times Cmatch3 \times W1$$

$$VB2 = Cmatch2 \times Cmatch3 \times Ldeg \times Lmatch1 \quad (4.2)$$

$$VB1 = Cmatch1 \times Cmatch3 \times Ldeg \times L1.$$

We run experiments four times. The experiments of the first three times we are devoted to achieving S22 to the target by the passive devices and keep other responses in the specification, because the response of S22 is far from the initial value to the target. Therefore

Table 4.4: A list of the results of the predicted values after optimization in the first three experiments using CCF design.

Response	S11	S12	S21	S22	K	NF	IIP3
Goals	< -10dB	< -25dB	maximize	< -10dB	> 1	< 2	> -10
Original	-8.756dB	-39.2dB	13.38dB	-6.137dB	7.199	1.018	-8.17
Experiment 1	-17.39dB	-38.57dB	14.02dB	-8.281dB	7.377	0.8925	-7.805
Experiment 2	-19.88dB	-38.27dB	13.89dB	-10.15dB	7.705	0.9365	-6.985
Experiment 3	-18.03dB	-38.04dB	13.8dB	-12.72dB	7.874	0.9674	-6.58

we have three experiments to make these range of all responses include our targets. Table 4.4 shows the results of the above work in the first three experiments.

Finally we take the values of 10 factors after optimization in the 3th experimental as our nominal case. The experiment levels of 10 factors are shown in Tab. 4.5. We will discuss in the next section.

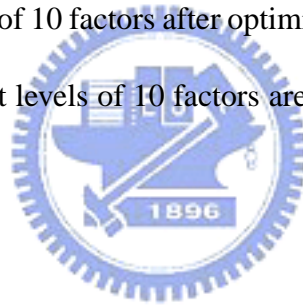


Table 4.5: Experiment levels for 10 factors after optimization of the 3th experiment .

Factor name	Center value	Cube (± 1)	Axial ($\pm\alpha = \pm 1$)
A: Cmatch1 (F)	764.9	$\pm 10\%$	$\pm 10\%$
B: Cmatch2 (P)	2.048	$\pm 5\%$	$\pm 5\%$
C: Cmatch3 (P)	3.28	$\pm 5\%$	$\pm 5\%$
D: Ldeg (N)	1.22	$\pm 10\%$	$\pm 10\%$
E: Lmatch1 (N)	5.41	$\pm 10\%$	$\pm 10\%$
F: L1 (μm)	0.25	± 0.01	± 0.01
G: W1 (μm)	5	± 0.5	± 0.5
H: VB1 (V)	0.75	$\pm 10\%$	$\pm 10\%$
J: VB2 (V)	2.7	$\pm 4.5\%$	$\pm 4.5\%$
K: VDD (V)	2.7	$\pm 4.5\%$	$\pm 4.5\%$

4.2.2 The Response Surface Model

149 runs are completed to generate the necessary data for construction of the quadratic response models. Table 4.6 is the information for these 7 response surface models with an average R^2 value of 0.9825. In order to select significant effect we use the stepwise regression. The values F_{IN} and F_{OUT} are both set 0.1, and when the models are not hierarchical, we would add several insignificant terms to keep the hierarchy. The hierarchical ordering principle suggests that when resources are scarce, priority should be given to the estimation of lower order effects [37]. This is also a proper method to us because we don't want to lose any potential significant main effects.

In model adequacy checking, S11 and IIP3 have to be transformed by BOX-COX transformation or experience where Sec. 2.5 have introduced. The information for these 7 response surface models with stepwise regression are shown in Tab. 4.7, which are with an average R^2 value of 0.9893. Tables 4.8-4.14 show the significance of effect from large term to small one and coefficients of the response surface models with coded factors. The residual normal probability plots and scatter plots of these 7 responses are shown in the next section which also includes the results of two transformed responses.

Table 4.6: The information of 7 response surface models for the LNA circuit using CCF design.

Response	R^2	Adj. R^2	Std. Dev.
S11	0.9168	0.8493	1.38
S12	0.9957	0.9922	0.046
S21	0.9990	0.9982	0.04
S22	0.9905	0.9828	0.17
K	0.9994	0.9990	0.026
NF	0.9932	0.9876	0.017
IIP3	0.9827	0.9687	0.46

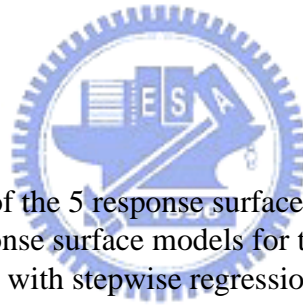


Table 4.7: The information of the 5 response surface models and 2 transformed response surface models for the LNA circuit using CCF design with stepwise regression method.

Response	R^2	Adj. R^2	Std. Dev.
1/S11	0.9608	0.9534	5.075E-5
S12	0.9947	0.9932	0.043
S21	0.9988	0.9984	0.038
S22	0.9889	0.9866	0.15
K	0.9994	0.9992	0.022
NF	0.9921	0.9908	0.015
$\log(IIP3 + 11.1265)$	0.9901	0.9867	0.026

Table 4.8: The coefficients of $1/S_{11}$ with coded factors in a significance order of the stepwise regression.

Factor	Coefficient	Factor	Coefficient	Factor	Coefficient
EG	-0.030	EF	-4.135E-3	FG	-1.281E-3
E^2	-0.011	DH	-2.379E-3	B	1.089E-3
AE	-9.849E-3	F	1.905E-3	G^2	-6.376E-3
EH	9.541E-3	E	1.740E-3	FH	9.923E-4
G	9.018E-3	AH	1.556E-3	DF	8.496E-4
DE	7.080E-3	AG	1.371E-3	GH	8.013E-4
A	-4.150E-3	AD	1.302E-3	DG	7.542E-4

Table 4.9: The coefficients of S_{12} with coded factors in a significance order of the stepwise regression.

Factor	Coefficient	Factor	Coefficient	Factor	Coefficient
G	0.42	EG	-0.072	FG	-0.028
K	-0.14	DE	0.061	BC	-0.026
GH	0.14	DH	0.059	AH	0.023
D	0.11	DG	0.057	H^2	0.058
H	-0.10	J	-0.052	E^2	-0.14
F	-0.094	HK	-0.046	AG	0.018
E	-0.093	HJ	0.036	AD	0.016
C	-0.091	JK	-0.032	GJ	0.013
EH	0.079	EF	-0.031	BE	0.011
AE	-0.078	B	-0.031	EJ	8.728E-3
A	-0.074	FH	-0.028	DJ	6.653E-3

Table 4.10: The coefficients of S21 with coded factors in a significance order of the stepwise regression.

Factor	Coefficient	Factor	Coefficient	Factor	Coefficient
H	0.82	C	-0.040	AB	0.014
D	-0.44	EF	-0.037	EJ	0.014
F	-0.22	G	-0.029	DF	0.013
H^2	-0.48	H^2	-0.24	DG	0.012
AE	-0.10	AH	0.025	JK	0.011
EH	0.090	HJ	-0.024	DJ	-0.011
EG	-0.083	GH	-0.022	FG	-0.011
B	0.073	BE	0.020	CH	-8.549E-3
DE	0.061	AD	0.019	HK	7.059E-3
A	-0.054	J	0.018	BH	-6.604E-3
K	0.050	BC	-0.017	E	6.027E-3
FH	0.046	E^2	-0.14	BG	5.738E-3
DH	-0.042	AG	0.016	BK	5.573E-3

Table 4.11: The coefficients of S22 with coded factors in a significance order of the stepwise regression.

Factor	Coefficient	Factor	Coefficient	Factor	Coefficient
C	0.97	K	-0.15	DE	-0.049
BC	0.74	BJ	0.15	DJ	-0.039
B^2	0.96	AB	-0.12	GH	0.031
BK	-0.25	BG	0.12	BH	0.031
H	0.23	BD	-0.097	BF	-0.026
B	-0.21	J	0.082	BE	-0.026
E	0.16	AG	-0.078	A	0.022
G	0.16	AH	-0.060		

Table 4.12: The coefficients of K with coded factors in a significance order of the stepwise regression.

Factor	Coefficient	Factor	Coefficient	Factor	Coefficient
H	-0.68	FH	-0.023	EF	6.271E-3
F	0.31	HJ	-0.023	DE	-6.162E-3
D	0.30	DF	0.021	AH	-5.526E-3
G	-0.23	JK	0.020	D^2	-0.030
K	0.098	EH	-0.019	DK	4.518E-3
DH	-0.088	J	0.016	FJ	4.305E-3
E	0.075	AE	0.015	AG	-4.142E-3
GH	-0.055	A	0.014	FG	-3.836E-3
DG	-0.047	H^2	0.033		
HK	0.030	GJ	-8.556E-3		

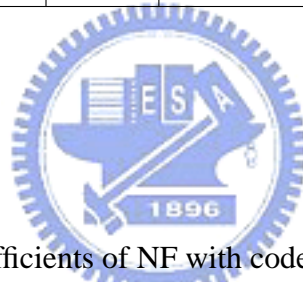


Table 4.13: The coefficients of NF with coded factors in a significance order of the stepwise regression.

Factor	Coefficient	Factor	Coefficient	Factor	Coefficient
H	-0.13	AE	0.024	AH	-7.248E-3
E	0.049	A	0.019	DE	-5.120E-3
F	0.042	EH	-0.014	H^2	0.041
C^2	0.096	EF	0.012	E^2	0.028
G	0.034	J	-0.012	HJ	2.935E-3
EG	0.033	FH	-0.011	EJ	-2.183E-3
D	0.028	FG	7.339E-3		

Table 4.14: The coefficients of IIP3 with coded factors in a significance order of the stepwise regression.

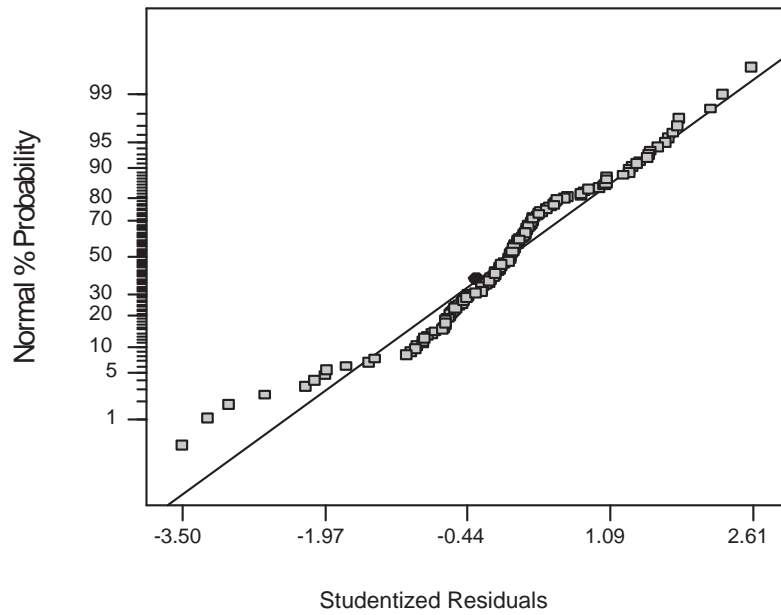
Factor	Coefficient	Factor	Coefficient	Factor	Coefficient
K	0.15	BK	-0.012	CH	6.803E-3
J	-0.14	AE	0.011	EJ	6.624E-3
H	-0.082	BJ	0.011	CK	-6.674E-3
D	0.061	EK	-0.010	BD	-5.666E-3
JK	0.035	DE	-0.010	AJ	5.255E-3
E	0.025	H^2	0.029	AK	-5.171E-3
F	0.025	BC	9.066E-3	GH	4.779E-3
A	0.019	HK	8.074E-3	GK	-4.788E-3
G	0.014	DJ	8.034E-3	FJ	4.283E-3
BH	0.014	DK	-7.981E-3	FK	-4.204E-3
EG	0.013	HJ	-7.126E-3	AD	-4.084E-3
DH	0.013	CJ	6.856E-3		

4.2.3 Summary

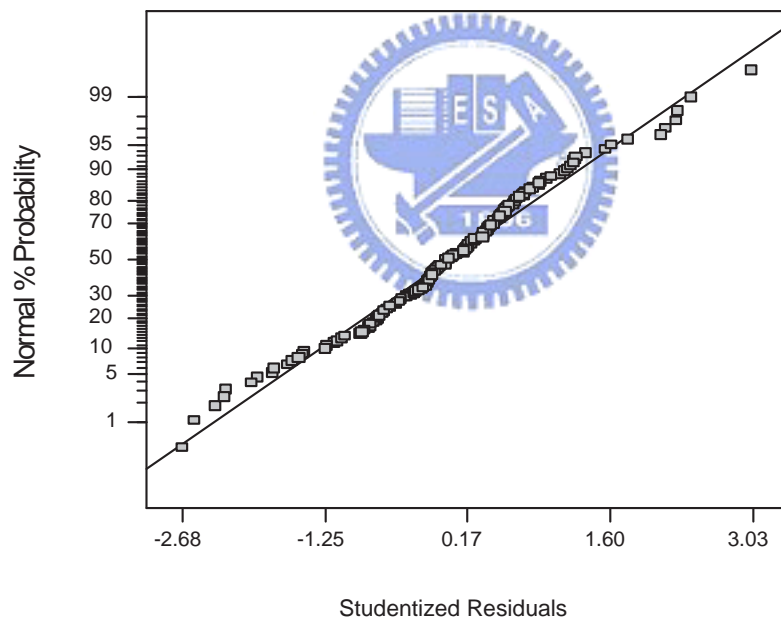
In this section, we provide the information of the 7 responses for the LNA circuit using the CCF design. Transformation of S11 and IIP3 by BOX-COX transformation or experience improves the model adequacy. We also provide the results of variable selection using the stepwise regression. Both the values F_{IN} and F_{OUT} are set to be 0.1, and we follow the hierarchical ordering principle. The R^2 , standard deviation, and coefficients of each response surface models are also obtained. The results of CCF design are deemed adequacy for continuously using in the circuit performance optimization algorithm and the sensitivity analysis.

4.3 Model Adequacy Checking

The residual normal probability plots, scatter plots of these 7 responses, and two transformed responses are shown in Figs. 4.8-4.16 where scatter plots of S11 and IIP3 reveal obvious pattern. After transformation of S11 and IIP3, the results confirm that the model assumption is satisfied.

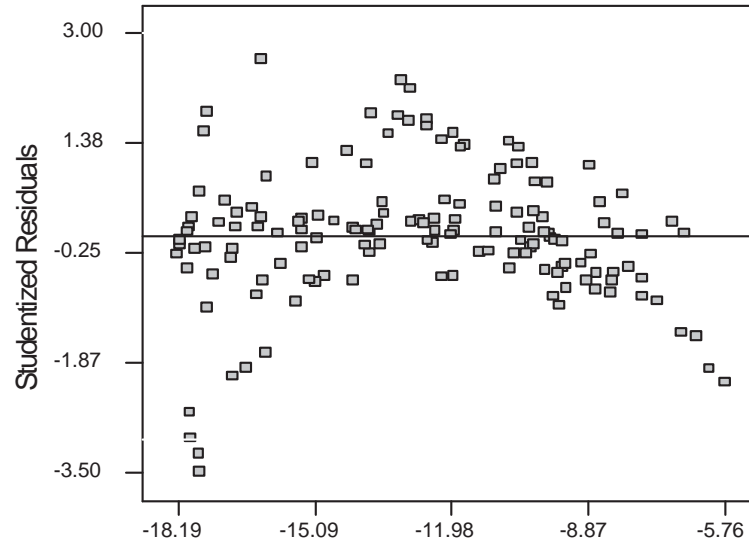


(a)



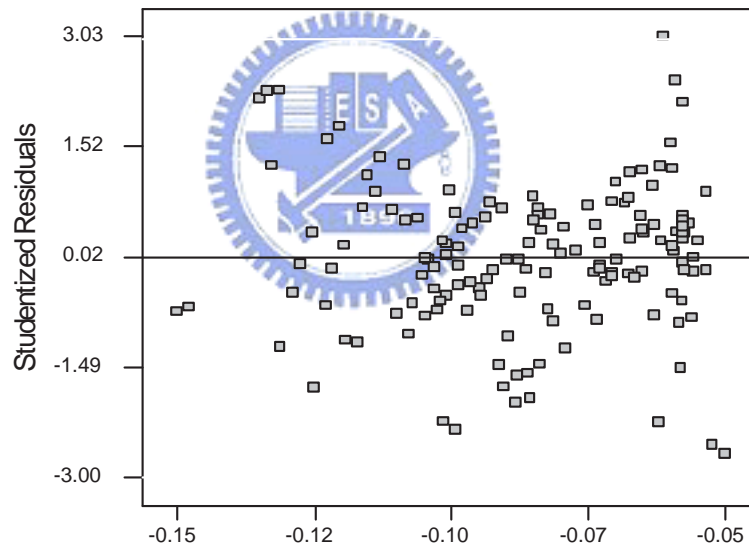
(b)

Figure 4.8: Residual normal probability plots for (a) S11 and (b) 1/S11.



Predicted

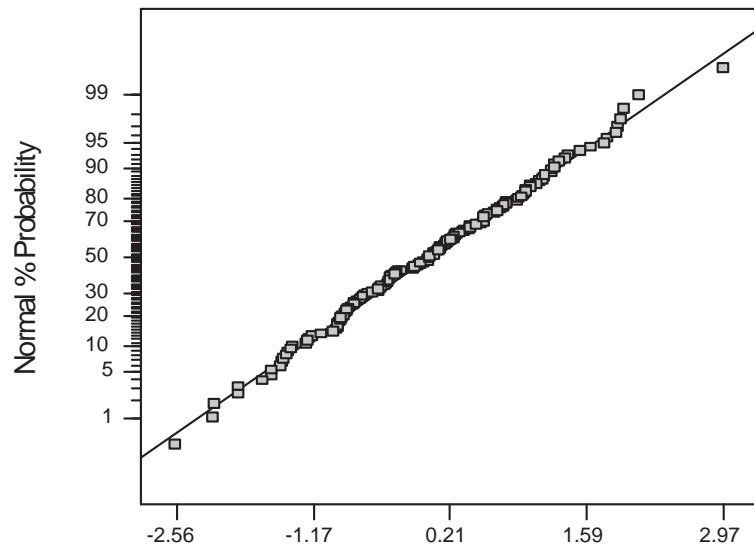
(a)



Predicted

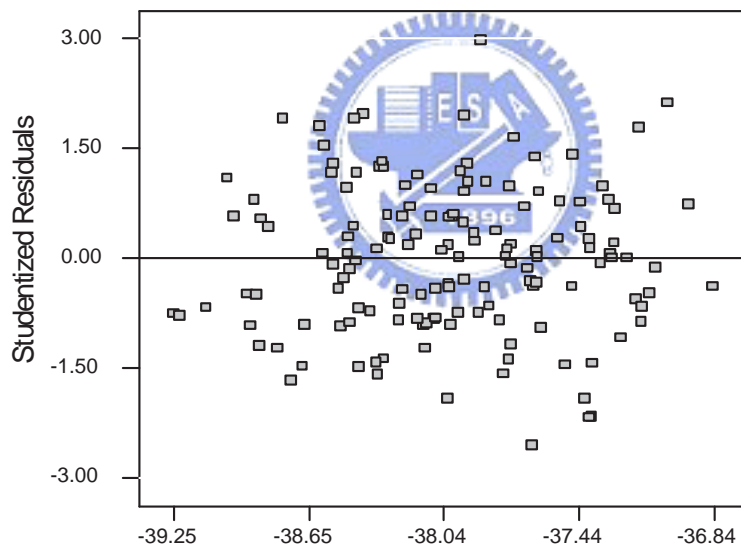
(b)

Figure 4.9: Residual scatter plots for (a) S11 and (b) 1/S11.



Studentized Residuals

(a)



Predicted

(b)

Figure 4.10: A model adequacy checking for S12 (a) residual normal probability plot and (b) the residual normal probability plot.

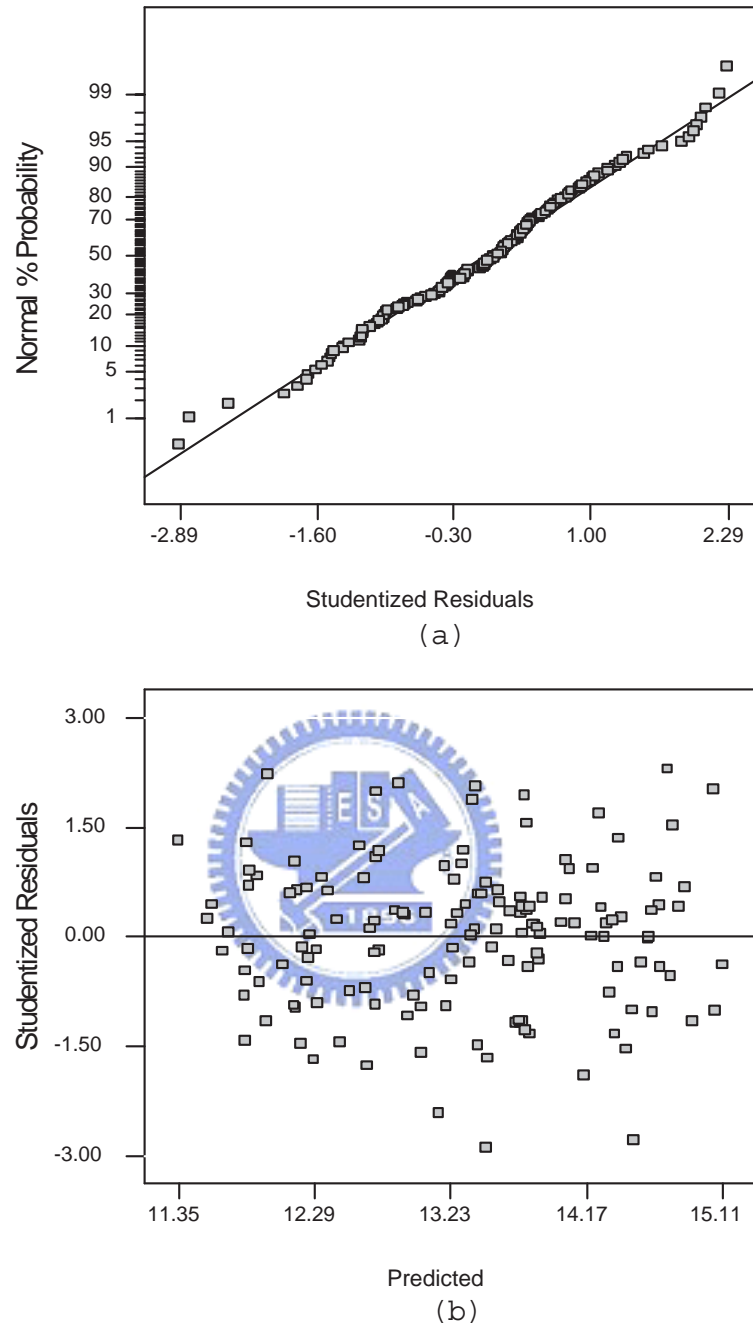
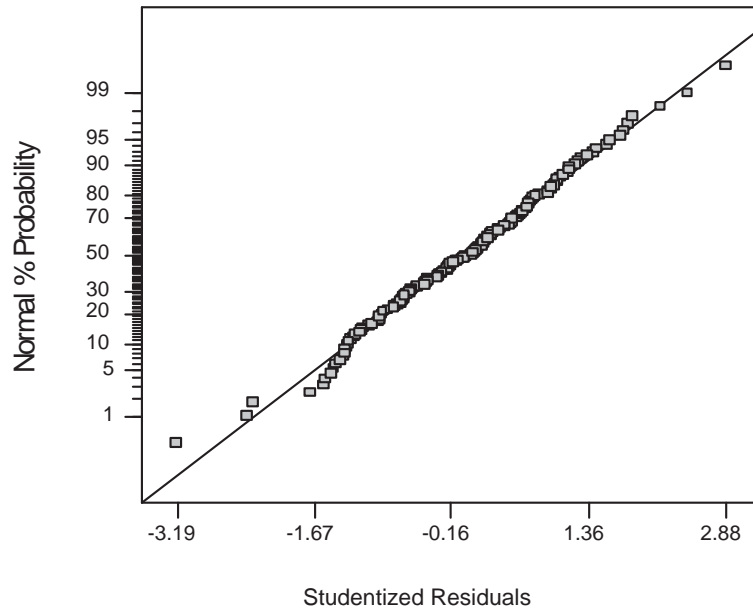
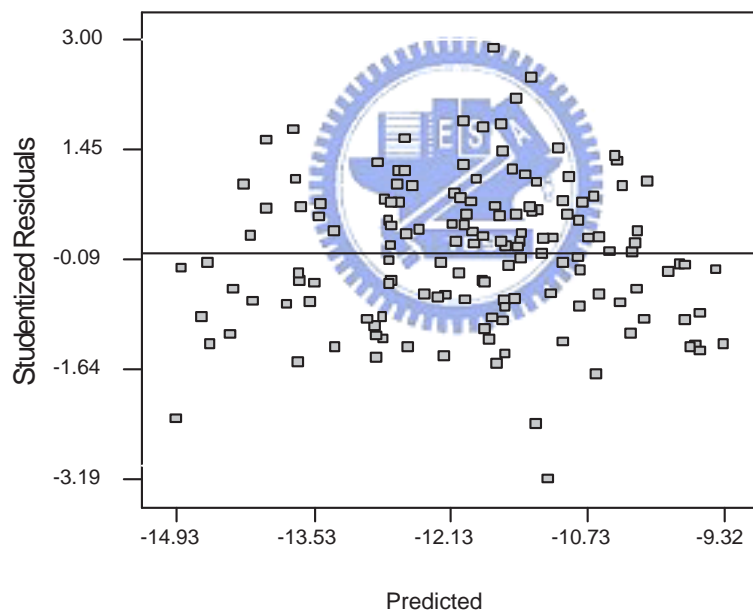


Figure 4.11: A model adequacy checking for S21 (a) residual normal probability plot and (b) the residual normal probability plot.

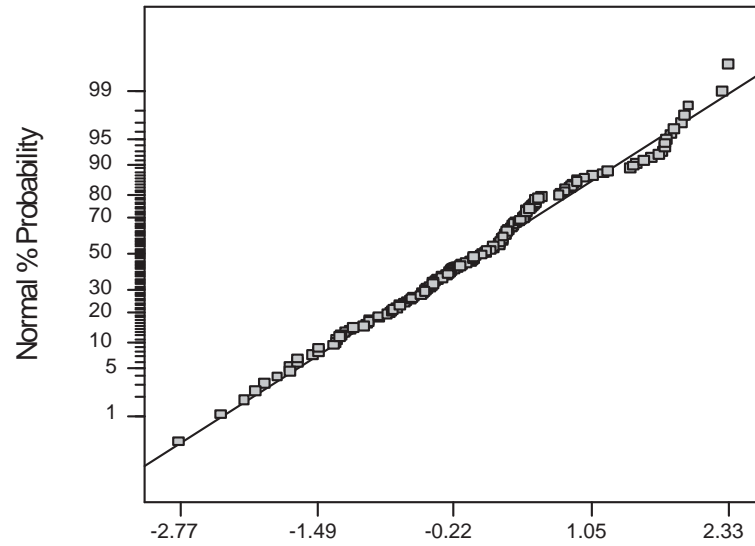


(a)



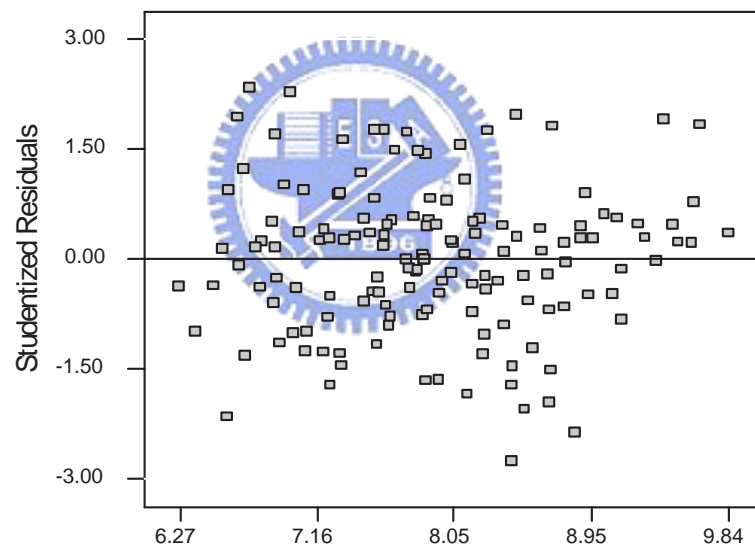
(b)

Figure 4.12: A model adequacy checking for S22 (a) residual normal probability plot and (b) the residual normal probability plot.



Studentized Residuals

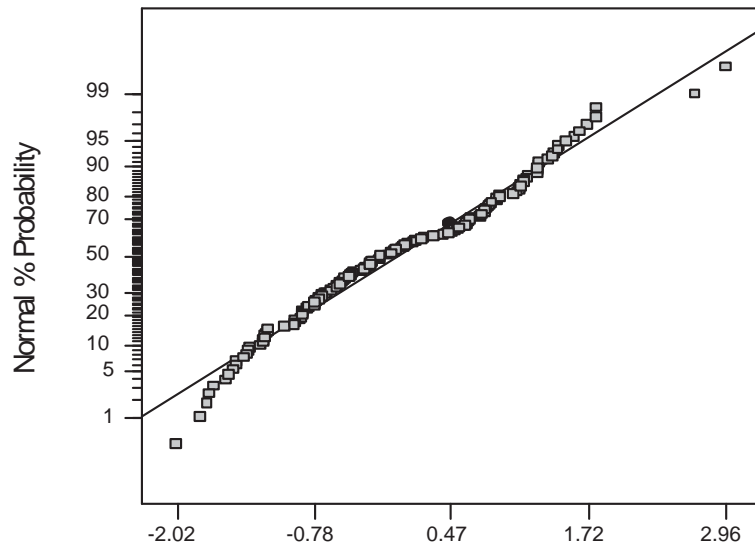
(a)



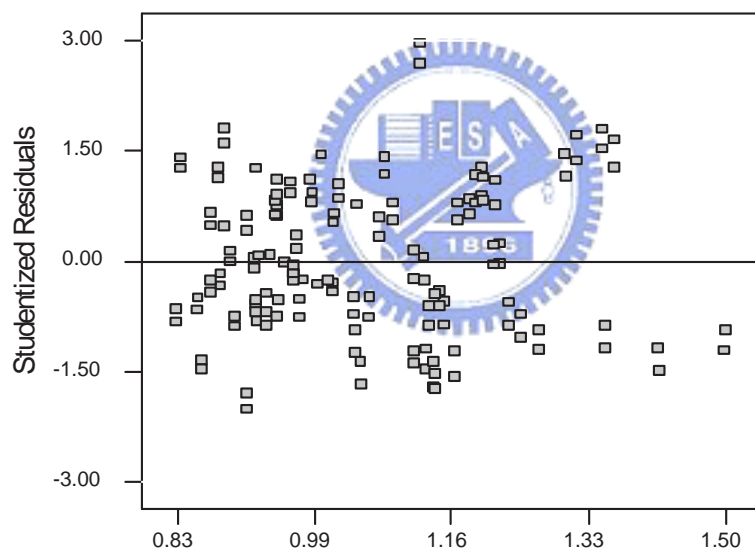
Predicted

(b)

Figure 4.13: A model adequacy checking for K (a) residual normal probability plot and (b) the residual normal probability plot.



(a)



(b)

Figure 4.14: A model adequacy checking for NF (a) residual normal probability plot and (b) the residual normal probability plot.

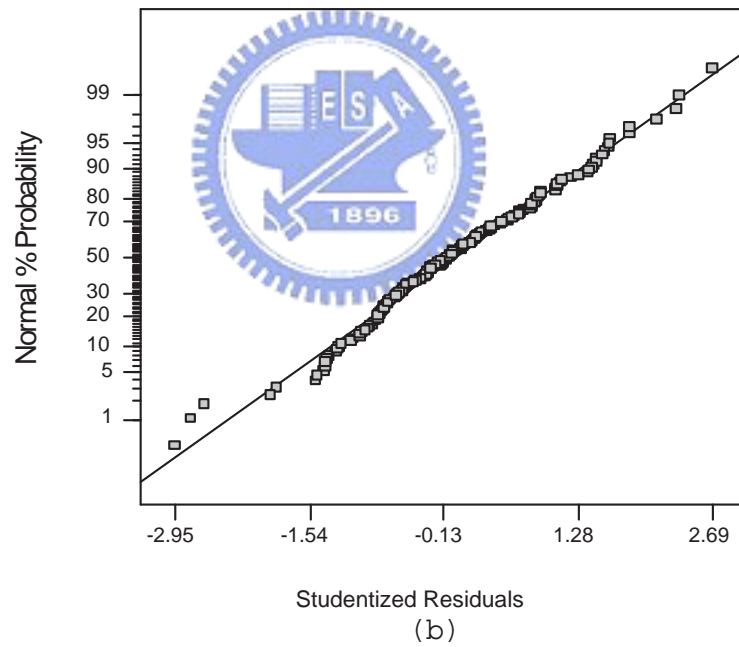
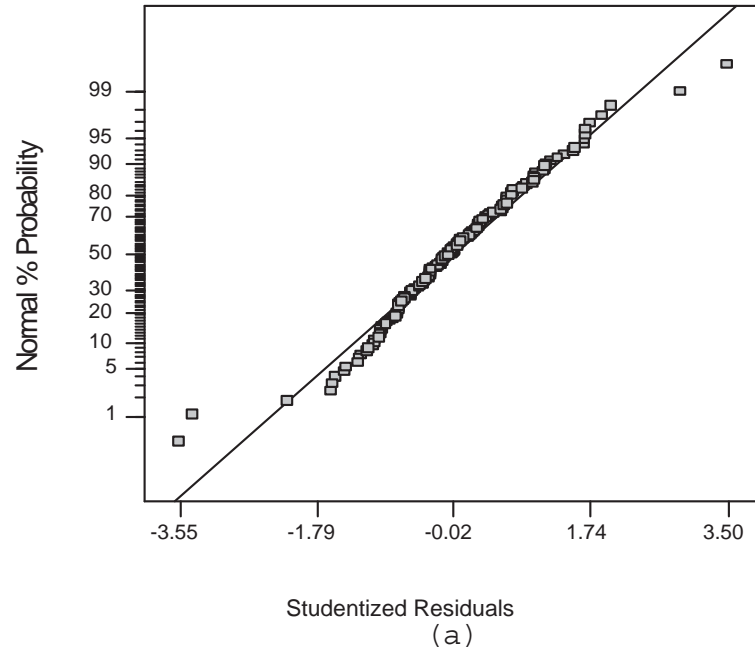
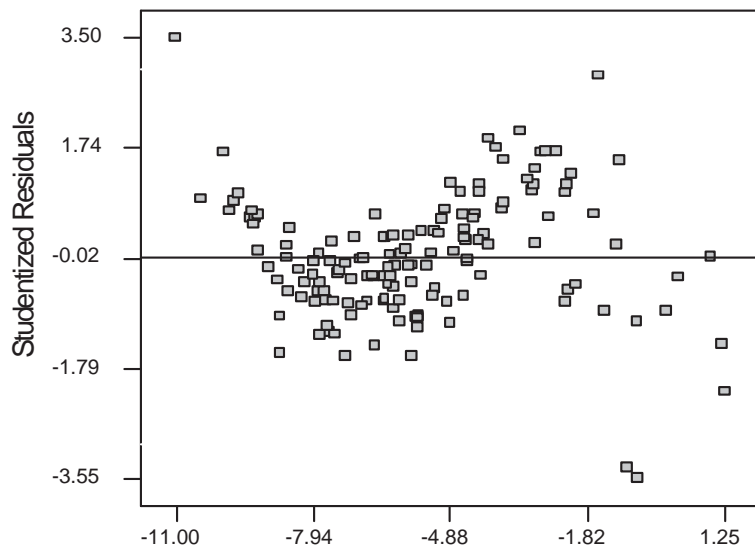
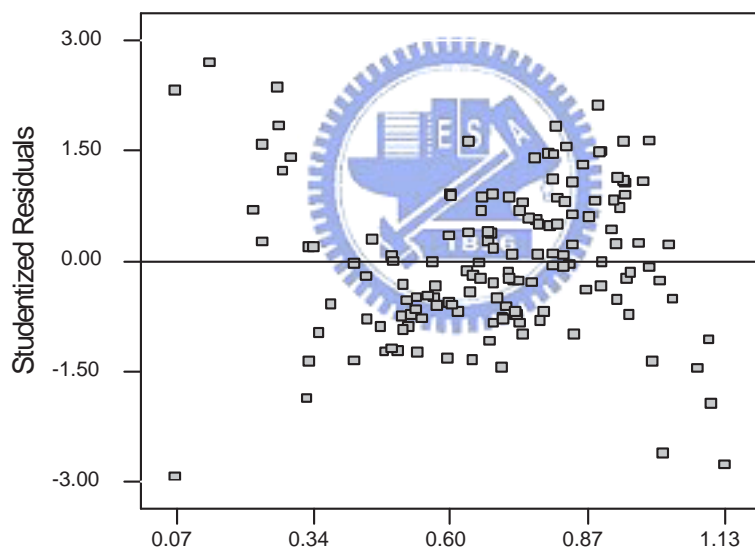


Figure 4.15: Residual normal probability plots for (a) IIP3 and (b) $\log(IIP3 + 11.1265)$.



Predicted
(a)



Predicted
(b)

Figure 4.16: Residual scatter plots for (a) IIP3 and (b) $\log(IIP3 + 11.1265)$.

4.3.1 Summary

The residual normal probability plots, scatter plots of these 7 responses and two transformed responses are discussed and shown in Figs. 4.8-4.16. And the two responses transformation improve the capability of explanation of the models.

4.4 Accuracy Verification

We have provided the 7 surface response models with stepwise regression in the previous section and the results of R^2 show that the models are well constructed according to the experimental design points of view. But the factor settings of optimization may not lie at the high (+1), low (-1), or zero factor level setting. We are interested in the accuracy of the 7 models within our high and low level settings, and we generate 100 random numbers for each factor with *uniform*(-1, 1) distribution. 100 random numbers are enough for the accuracy verification.

4.4.1 Accuracy Verification Results

The results calculated from the response surface models and circuit simulator are shown in Tab. 4.15 and Tab. 4.16. And the scatter plots of values calculated from the response

Table 4.15: Accuracy verification of the results calculated from the constructed response surface model.

Values calculated from response surface models	S11	S12	S21	S22	K	NF	IIP3
Mean	-15.12	-38.04	13.65	-12.33	7.84	0.9995	-6.26
Std. Dev.	2.40	0.31	0.55	0.79	0.48	0.090	1.48

surface models versus values that obtained from circuit simulator are shown in Figs. 4.17-4.23. The results show that there is a high linearity between actual and predicted values.

4.4.2 Summary

In this section, we generate 100 random numbers for each factor with $uniform(-1, 1)$ distribution to verify the accuracy of the 7 response surface models within our high and low level settings. The results are quite high linearity, and predicted values represent actual values enough.

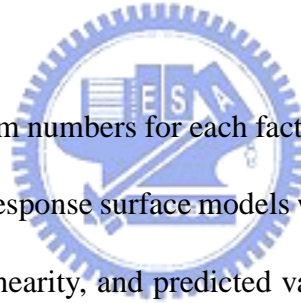


Table 4.16: Accuracy verification of the results obtained from circuit simulator.

Values calculated from circuit simulator	S11	S12	S21	S22	K	NF	IIP3
Mean	-14.92	-38.05	13.66	-12.31	7.85	0.9952	-6.20
Std. Dev.	3.30	0.32	0.54	1.017	0.49	0.088	1.63

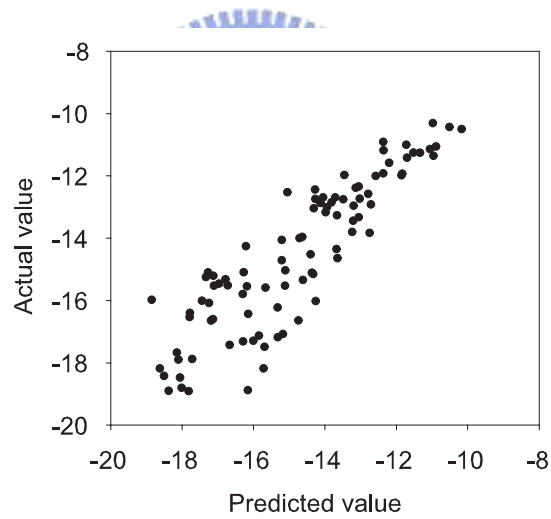


Figure 4.17: A scatter plot calculated from the response surface model versus values obtained from circuit simulator for S11.

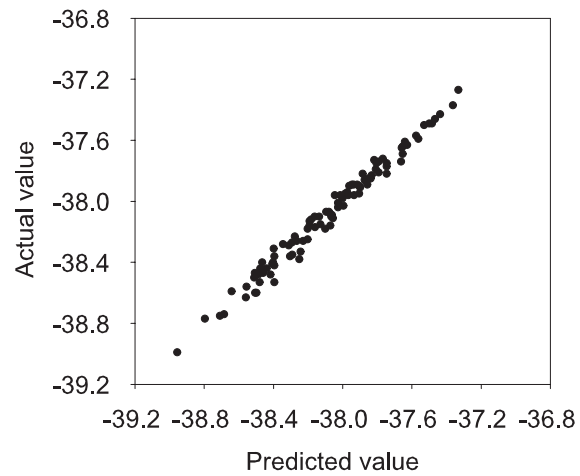


Figure 4.18: A scatter plot calculated from the response surface model versus values obtained from circuit simulator for S12.

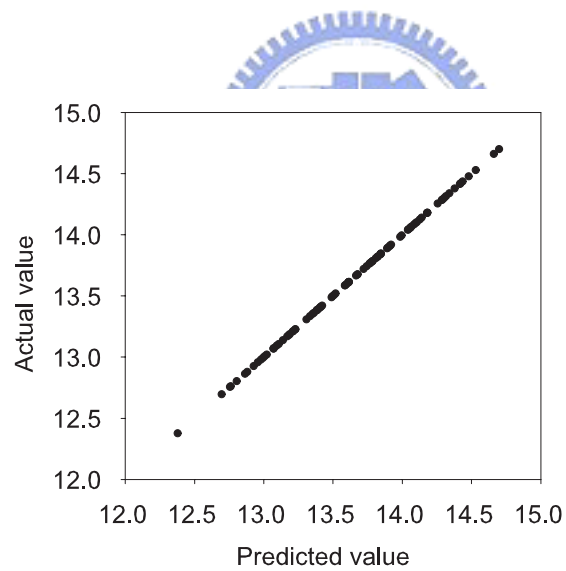


Figure 4.19: A scatter plot calculated from the response surface model versus values obtained from circuit simulator for S21.

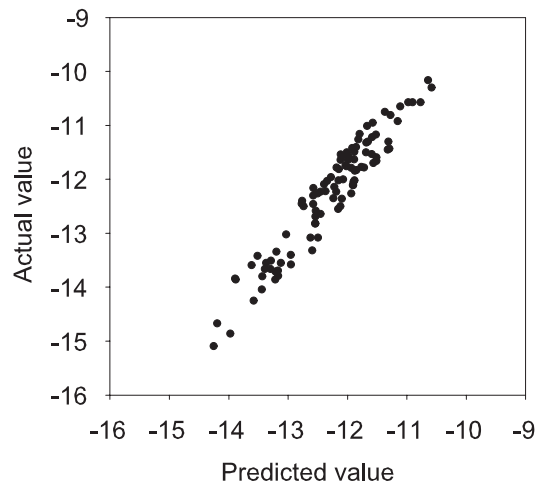


Figure 4.20: A scatter plot calculated from the response surface model versus values obtained from circuit simulator for S22.

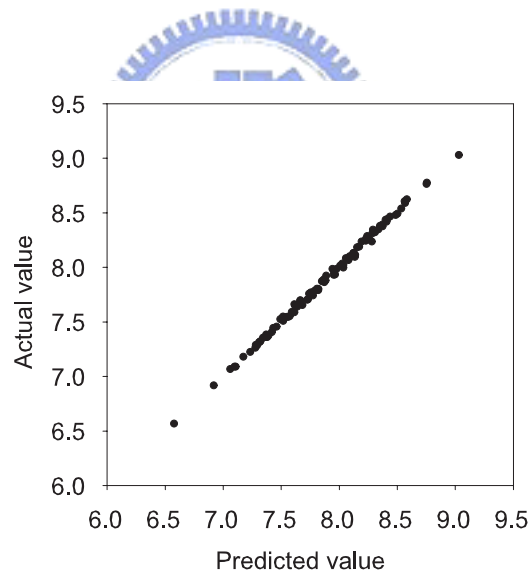


Figure 4.21: A scatter plot calculated from the response surface model versus values obtained from circuit simulator for K.

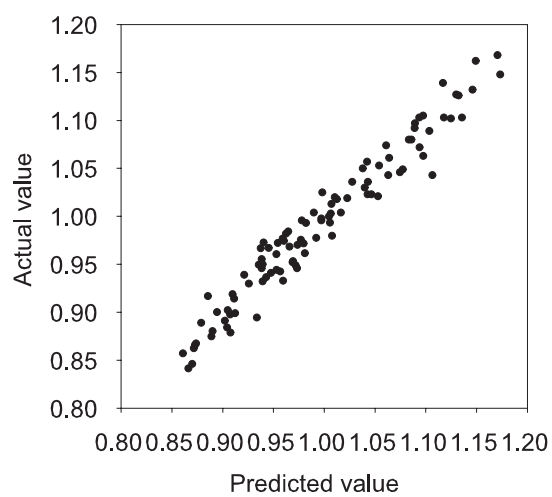


Figure 4.22: A scatter plot calculated from the response surface model versus values obtained from circuit simulator for NF.

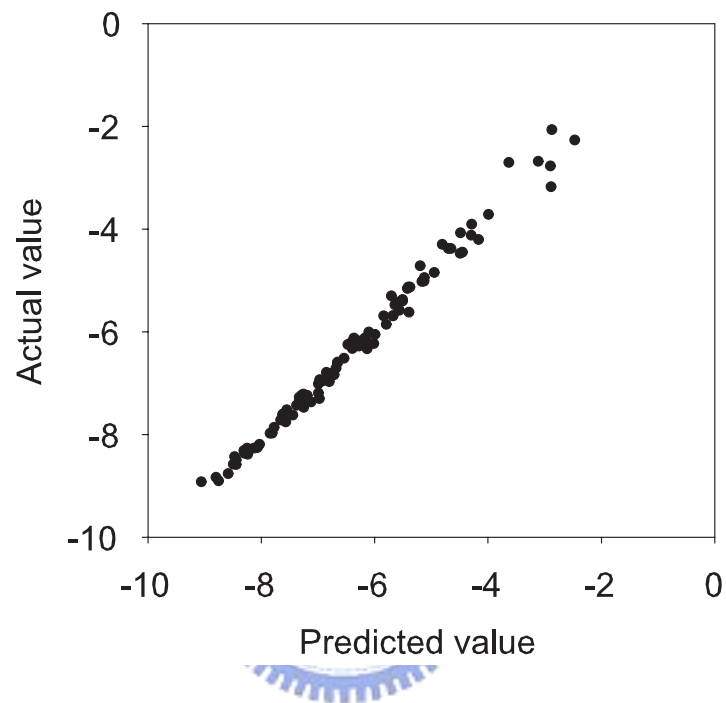


Figure 4.23: The scatter plots of values calculated from response surface models versus values obtained from circuit simulator for IIP3.

Chapter 5

LNA Circuit Design Optimization

To achieve optimization of the LNA circuit performance automatically, we use Design Expert® to proceed this work, where a numerical method is applied. 2^{nd} order response surface model with the stepwise regression method is applied. Table 5.1 presents the constraints of the circuit parameters, and Tab. 5.2 displays the response targets for the optimization.

Table 5.1: The constraints of LNA circuit parameters.

Parameter	Lower limit	Upper limit
A: Cmatch1 (F)	688.4	841.4
B: Cmatch2 (P)	1.946	2.150
C: Cmatch3 (P)	3.12	3.44
D: Ldeg (N)	1.10	1.35
E: Lmatch1 (N)	4.87	5.95
F: L1 (μm)	0.24	0.26
G: W1 (μm)	4.5	5.5
H: VB1 (V)	0.675	0.825
J: VB2 (V)	2.5785	2.8215
K: VDD (V)	2.5785	2.8215



Table 5.2: The targets of responses.

Response	Goal	Lower limit	Upper limit
S11	$< -10\text{dB}$	-21.32	-6.63
S12	$< -25\text{dB}$	-39.28	-36.85
S21	maximize	11.39	15.12
S22	$< -10\text{dB}$	-15.25	-9.44
K	> 1	6.26	9.85
NF	< 2	0.82	1.481
IIP3	> -10	-10.12	0.94

5.1 Optimization Results Using the Stepwise Regression

Models

There are three optimized cases which satisfy all specifications, minimize the noise figure, and maximize the voltage gain. In the the process of the optimization we modify the specifications by $2\hat{\sigma}$ to ensure the recipes are 95 % credible. Firstly, according to the objective function which is presented in Eqs. 2.23, 2.24, 2.25, and 2.26, the seven responses are transformed into their individual desirabilities. These individual desirabilities are then combined using geometric mean to get the desirability function D . Therefore we maximize the desirability function to get optimal recipes. The constraint of the three optimized cases are shown in Tabs. 5.3-5.5. In the case of satisfied all specifications, the upper and lower weight are equal to 1. In the case of minimized noise figure, the upper weight is equal to 10, that means more important to minimize noise figure. In the case of maximized voltage gain, the lower weight is equal to 10, that means more important to maximize voltage gain. The upper or lower limit are also considering their specifications and modify the specifications by $2\hat{\sigma}$ when the target is out of the specifications.

Tables 5.6-5.8 show the original case and the three optimal recipes for these three cases. Design Expert® uses direct search methods to maximize the desirability function D . Tables 5.9-5.11 provide the predicted responses for the three cases which are estimated by

Table 5.3: The constraint for the case of satisfied all specifications. We modify the specifications within $2\hat{\sigma}$.

Response	Goal	Lower limit	Upper Limit	Lower weight	Upper weight
S11 (dB)	minimize	-21.32	-10	1	1
S12 (dB)	minimize	-39.28	-39.2	1	1
S21 (dB)	maximize	13.456	15.12	1	1
S22 (dB)	minimize	-15.25	-10.3	1	1
K	maximize	7.199	9.846	1	1
NF (dB)	minimize	0.816	1.018	1	1
IIP3 (dB)	maximize	-8.17	0.94	1	1

the response surface models with the stepwise regression method, and the completed contour plots are provided in Appendix A for one case. Tables 5.12-5.14 provide the actual responses for the three cases which are obtained by running circuit simulator. We can observe that the predicted optimal recipes are accurate. Next we discuss three cases in detail, and the results of three optimized cases are better than that of the original cases.

Table 5.4: The constraint for the case of minimized noise figure. We modify the specifications within $2\hat{\sigma}$.

Response	Goal	Lower limit	Upper Limit	Lower weight	Upper weight
S11 (dB)	minimize	-21.32	-10	1	1
S12 (dB)	minimize	-39.28	-36.85	1	1
S21 (dB)	maximize	11.39	15.12	1	1
S22 (dB)	minimize	-15.25	-10.3	1	1
K	maximize	6.262	9.846	1	1
NF (dB)	minimize	0.816	1.482	1	10
IIP3 (dB)	maximize	-9.948	0.94	1	1



Table 5.5: The constraint for the case of maximized voltage gain. We modify the specifications within $2\hat{\sigma}$.

Response	Goal	Lower limit	Upper Limit	Lower weight	Upper weight
S11 (dB)	minimize	-21.32	-10	1	1
S12 (dB)	minimize	-39.28	-36.85	1	1
S21 (dB)	maximize	11.39	15.12	10	1
S22 (dB)	minimize	-15.25	-10.3	1	1
K	maximize	6.262	9.846	1	1
NF (dB)	minimize	0.816	1.482	1	1
IIP3 (dB)	maximize	-9.948	0.94	1	1

Table 5.6: Optimal recipes for the case of satisfied all specifications calculated by the 2nd order response surface model. "1" means the highest priority.

Recipe	Nominal case	1	2	3
Cmatch1 (F)	764.9	836.6	841.4	841.4
Cmatch2 (P)	2.048	2.045	2.124	2.074
Cmatch3 (P)	3.28	3.35	3.41	3.39
Ldeg (N)	1.22	1.10	1.11	1.10
Lmatch1 (N)	5.41	5.88	5.87	5.88
L1 (μm)	0.25	0.26	0.26	0.26
W1 (μm)	5	4.50	4.50	4.50
VB1 (V)	0.7	0.799	0.803	0.797
VB2 (V)	2.7	2.7427	2.7178	2.6405
VDD (V)	2.7	2.8214	2.7936	2.8215

Table 5.7: Optimal recipes for the case of minimized noise figure calculated by the 2nd order response surface model. "1" means the highest priority.

Recipe	Nominal case	1	2	3
Cmatch1 (F)	764.9	688.5	688.4	688.4
Cmatch2 (P)	2.048	2.096	2.111	2.097
Cmatch3 (P)	3.28	3.22	3.20	3.22
Ldeg (N)	1.22	1.10	1.21	1.10
Lmatch1 (N)	5.41	5.74	5.80	5.67
L1 (μm)	0.25	0.24	0.24	0.24
W1 (μm)	5	4.50	4.50	4.50
VB1 (V)	0.7	0.808	0.823	0.793
VB2 (V)	2.7	2.5785	2.6523	2.6090
VDD (V)	2.7	2.8215	2.8215	2.8207

Table 5.8: Optimal recipes for the case of maximized voltage gain calculated by the 2nd order response surface model. "1" means the highest priority.

Recipe	Nominal case	1	2	3
Cmatch1 (F)	764.9	688.4	688.4	688.7
Cmatch2 (P)	2.048	2.131	2.140	2.142
Cmatch3 (P)	3.28	3.15	3.19	3.13
Ldeg (N)	1.22	1.11	1.10	1.10
Lmatch1 (N)	5.41	5.90	5.81	5.86
L1 (μm)	0.25	0.25	0.25	0.25
W1 (μm)	5	4.50	4.50	4.50
VB1 (V)	0.7	0.825	0.828	0.825
VB2 (V)	2.7	2.6530	2.5797	2.7191
VDD (V)	2.7	2.8206	2.7875	2.8214

Table 5.9: Optimal results for the case of satisfied all specifications calculated by the 2nd order response surface model. "1" means the highest priority.

Values calculated from response surface models	Goal	1	2	3
S11 (dB)	< -10	-10.697	-10.846	-10.552
S12 (dB)	< -25	-39.266	-39.271	-39.227
S21 (dB)	maximized	14.351	14.314	14.325
S22 (dB)	< -10	-12.173	-11.242	-12.035
K	> 1	7.895	7.870	7.812
NF (dB)	< 2	0.946	0.962	0.961
IIP3 (dB)	> -10	-5.831	-5.801	-4.732
Desirability		0.404	0.382	0.356

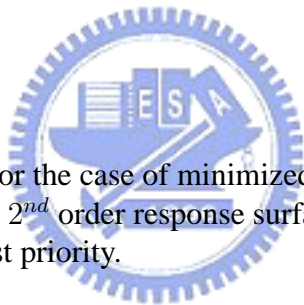


Table 5.10: Optimal results for the case of minimized noise figure calculated by the 2nd order response surface model. "1" means the highest priority.

Values calculated from response surface models	Goal	1	2	3
S11 (dB)	< -10	-16.578	-16.755	-16.319
S12 (dB)	< -25	-38.582	-38.478	-38.535
S21 (dB)	maximized	15.125	14.903	15.083
S22 (dB)	< -10	-13.408	-13.356	-13.453
K	> 1	7.272	7.370	7.256
NF (dB)	< 2	0.816	0.816	0.814
IIP3 (dB)	> -10	-5.031	-5.544	-5.404
Desirability		0.702	0.695	0.693

Table 5.11: Optimal results for the case of maximized voltage gain calculated by the 2nd order response surface model. "1" means the highest priority.

Values calculated from response surface models	Goal	1	2	3
S11 (dB)	< -10	-16.240	-16.915	-16.671
S12 (dB)	< -25	-38.654	-38.609	-38.687
S21 (dB)	maximized	15.12	15.12	15.12
S22 (dB)	< -10	-13.714	-13.333	-13.643
K	> 1	7.352	7.331	7.387
NF (dB)	< 2	0.839	0.833	0.842
IIP3 (dB)	> -10	-5.980	-5.530	-6.663
Desirability		0.706	0.702	0.702



Table 5.12: Optimal results for the case of satisfied all specifications by running circuit simulator. "1" means the highest priority.

Values obtained from circuit simulator	Goal	Originl	1	2	3
S11 (dB)	< -10	-8.756	-10.37	-10.54	-10.22
S12 (dB)	< -25	-39.2	-39.3	-39.32	-39.29
S21 (dB)	maximized	13.38	14.31	14.32	14.27
S22 (dB)	< -10	-6.137	-12.29	-11.07	-11.92
K	> 1	7.199	7.948	7.921	7.932
NF (dB)	< 2	1.018	0.980	0.980	0.993
IIP3 (dB)	> -10	-8.17	-5.73	-5.58	-4.21

Table 5.13: Optimal results for the case of minimized noise figure by running circuit simulator. "1" means the highest priority.

Values obtained from circuit simulator	Goal	Originl	1	2	3
S11 (dB)	< -10	-8.756	-18.13	-17.14	-17.57
S12 (dB)	< -25	-39.2	-38.49	-38.40	-38.50
S21 (dB)	maximized	13.38	15.17	14.85	15.07
S22 (dB)	< -10	-6.137	-13.39	-13.32	-13.41
K	> 1	7.199	7.157	7.341	7.254
NF (dB)	< 2	1.018	0.808	0.817	0.812
IIP3 (dB)	> -10	-8.17	-5.52	-5.67	-5.77

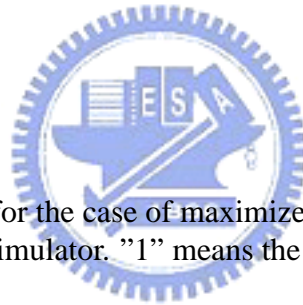


Table 5.14: Optimal results for the case of maximized voltage gain by running circuit simulator. "1" means the highest priority.

Values obtained from circuit simulator	Goal	Originl	1	2	3
S11 (dB)	< -10	-8.756	-17.34	-18.33	-17.95
S12 (dB)	< -25	-39.2	-38.66	-38.59	-38.68
S21 (dB)	maximized	13.38	15.09	15.11	15.14
S22 (dB)	< -10	-6.137	-13.60	-13.07	-13.53
K	> 1	7.199	7.413	7.325	7.389
NF (dB)	< 2	1.018	0.840	0.834	0.831
IIP3 (dB)	> -10	-8.17	-5.915	-5.55	-6.78

5.2 Comparison of Three Optimized Cases

The section we compare with three optimized cases which satisfy all specifications, minimize the noise figure, and maximize the voltage gain. Using the desirability function D we achieve the goals easily and we select the largest D as the example of the three cases. In the case of minimize the noise figure, the upper weight is equal to 10, that means we pay more attention to minimize the noise figure. In the case of maximize the voltage gain, the lower weight is equal to 10, that means we pay more attention to maximize the voltage gain.

Figure 5.1 shows comparison of the original case and three optimized cases for the result of S11 response. The result is acceptable if S11 parameter is smaller than -10 dB within the working region (2.11 GHz ~ 2.17 GHz). Figure 5.1 describes that the results of three optimized cases have achieved to this goal.

Figure 5.2 shows comparison of the original case and three optimized cases for the result of S12 response. The result is acceptable if S12 response is smaller than -25 dB within the working region. Figure 5.2 shows that the original case and the results of three optimized cases have achieved to this goal. Compared with the original case, the optimized result are slightly risen. This phenomenon is due to a compromise among response so that other responses can achieve their goal.

Figure 5.3 shows comparison of the original case and three optimized cases for the

result of S_{21} response. Although S_{21} response doesn't have critical criteria, to get the value as great as possible is good for LNA circuit design. Figure 5.3 describes that the results of three optimized cases that are made some improvement from the original case.

Figure 5.4 shows comparison of the original case and three optimized cases for the result of S_{22} response. As the same as parameter S_{22} , the result is acceptable if S_{22} response is smaller than -10 dB within working region. Figure 5.4 shows that the results of three optimized cases have achieved to this goal.

Figure 5.5 shows comparison of the original case and three optimized cases for the result of K response. The criteria of K factor is that it should be greater than 1 in working region. As shown in Fig. 5.5, the original case has achieved this criteria, and the results of three optimized cases are made improvement from the original data.

Figure 5.6 shows comparison of the original case and three optimized cases for the result of NF response. The criteria of noise figure is that it should be smaller than 2 in working region. Figure 5.6 describes that original case and the results of three optimized cases have achieved to this goal and the results are improved from the original case.

Figure 5.7 shows comparison of original case and three optimized cases for the result of input intercept point 3rd. The criteria of $IIP3$ is that drop from peak to bottom should be greater than -20 dB and as small as possible. As shown in Fig. 5.7, the original case has achieved this criteria, and the optimized result does do an improvement from the original

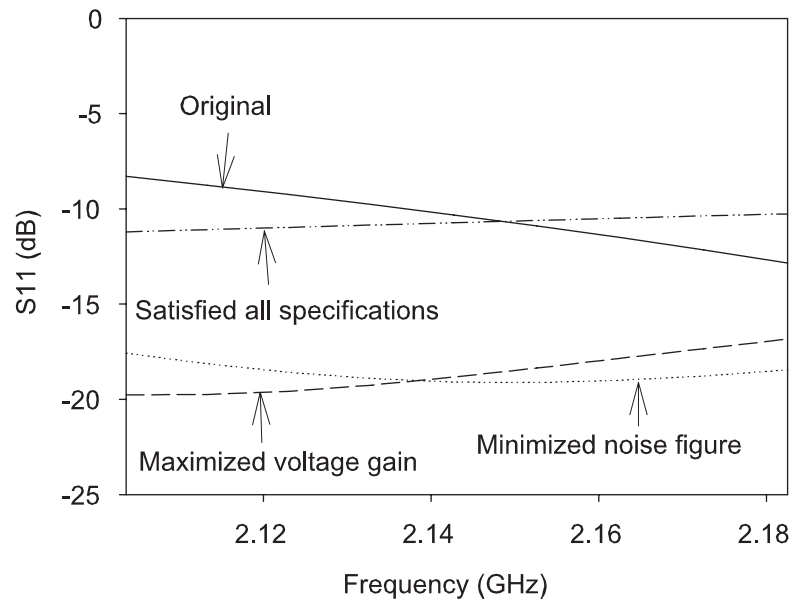


Figure 5.1: Comparison of original case and three optimized cases for the result of S11 response. A zoom-in plot for the operation frequency.

case.

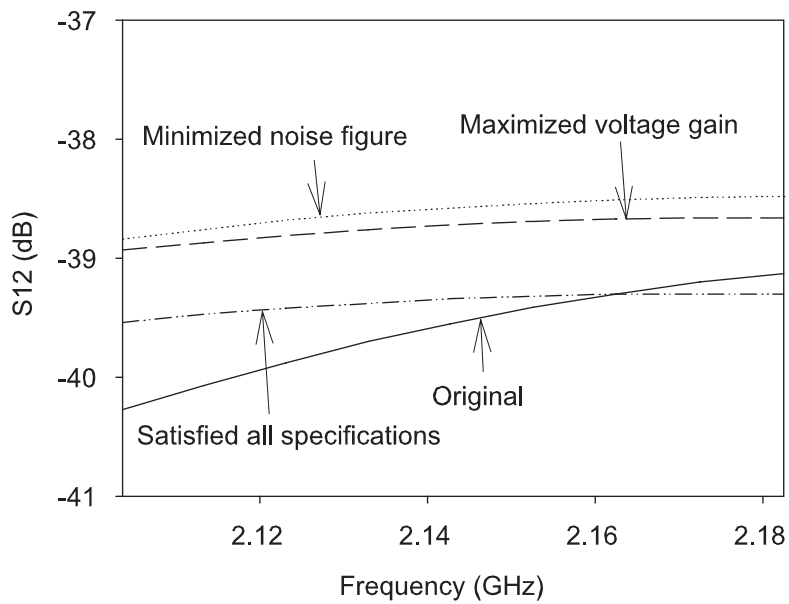


Figure 5.2: Comparison of original case and three optimized cases for the result of S12 response. A zoom-in plot for the operation frequency.

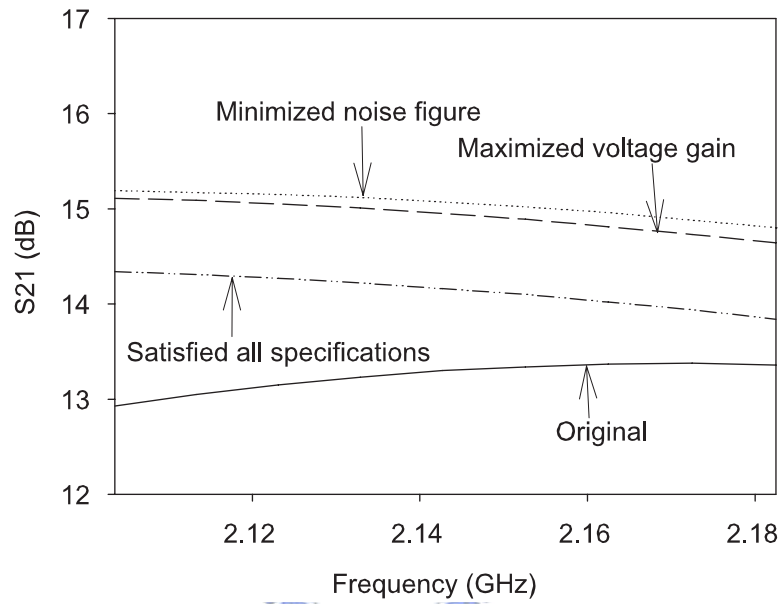


Figure 5.3: Comparison of original case and three optimized cases for the result of S21 response. A zoom-in plot for the operation frequency.

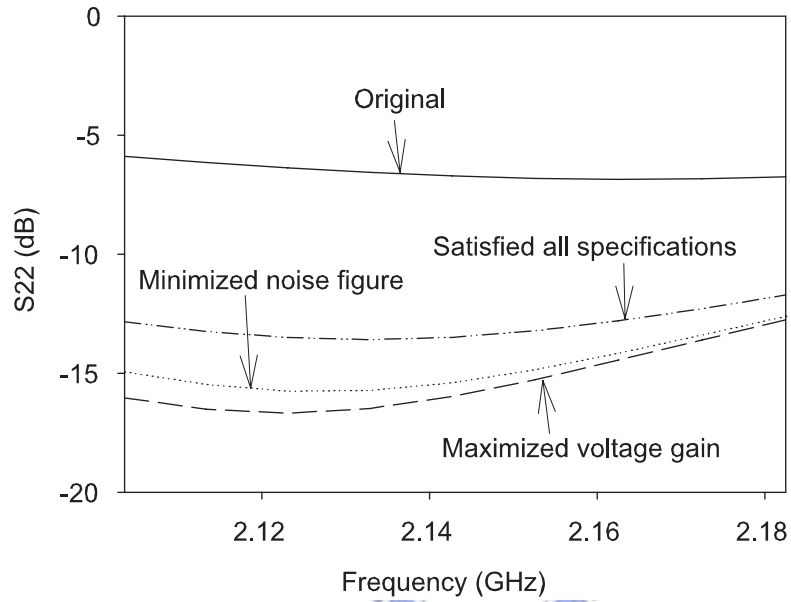


Figure 5.4: Comparison of original case and three optimized cases for the result of S22 response. A zoom-in plot for the operation frequency.

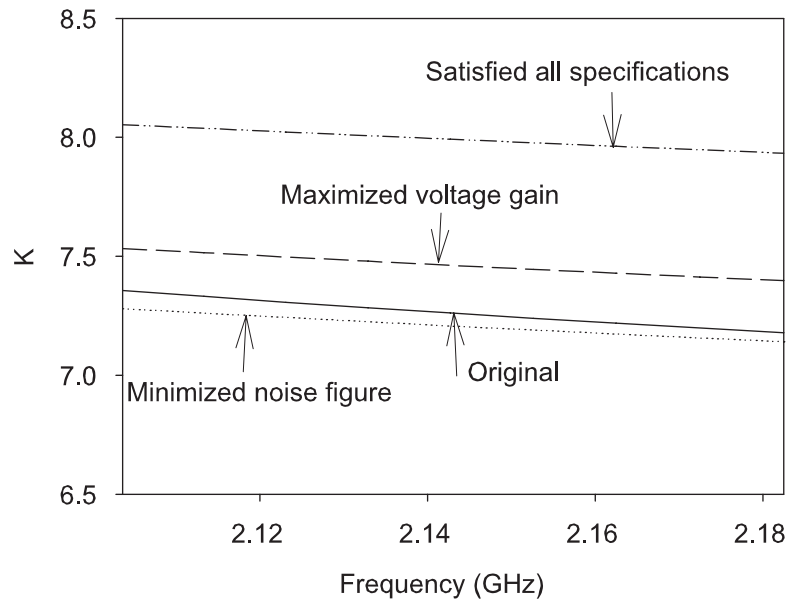


Figure 5.5: Comparison of original case and three optimized cases for the result of K response. A zoom-in plot for the operation frequency.

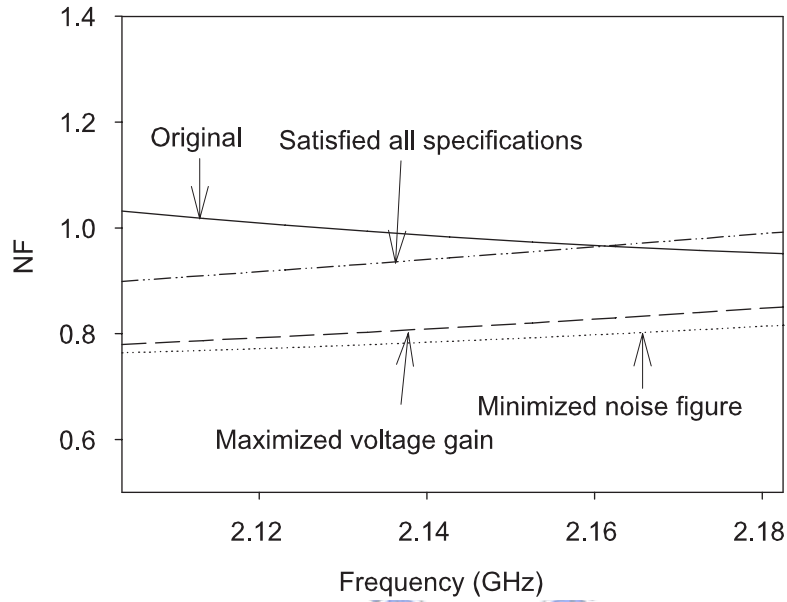
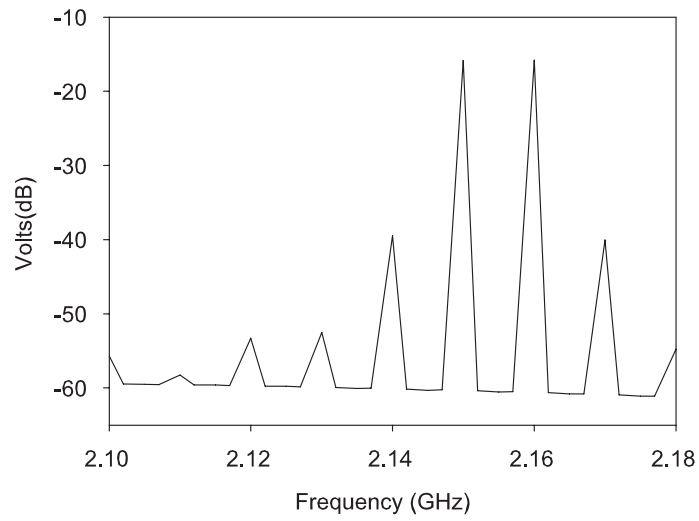
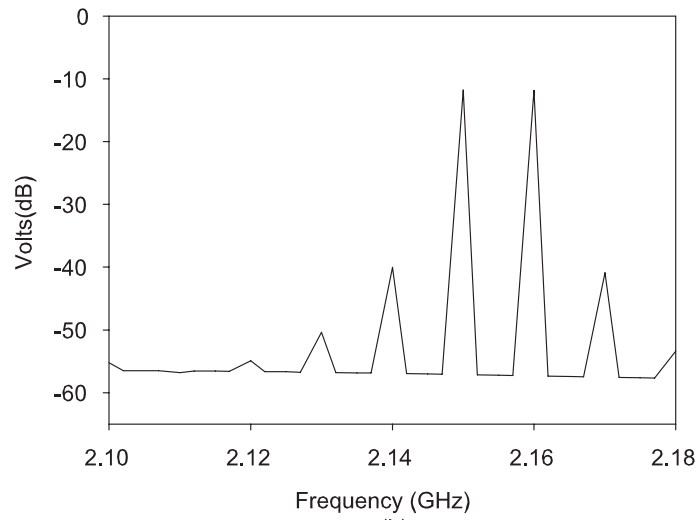


Figure 5.6: Comparison of original case and three optimized cases for the result of NF response. A zoom-in plot for the operation frequency.



(a)



(b)

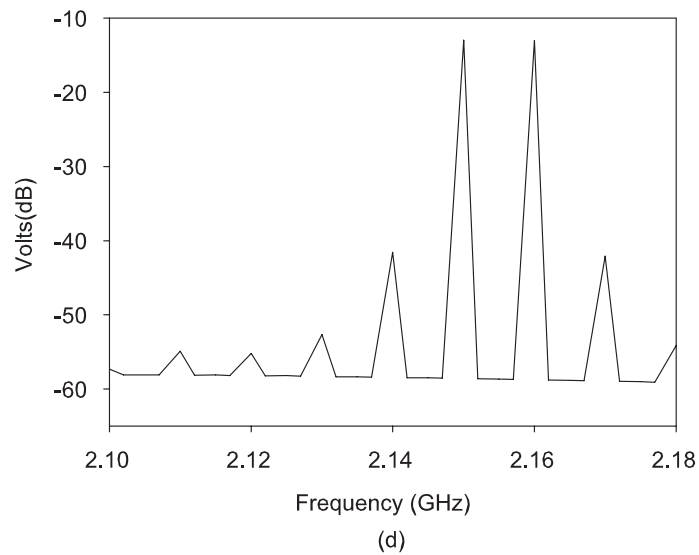
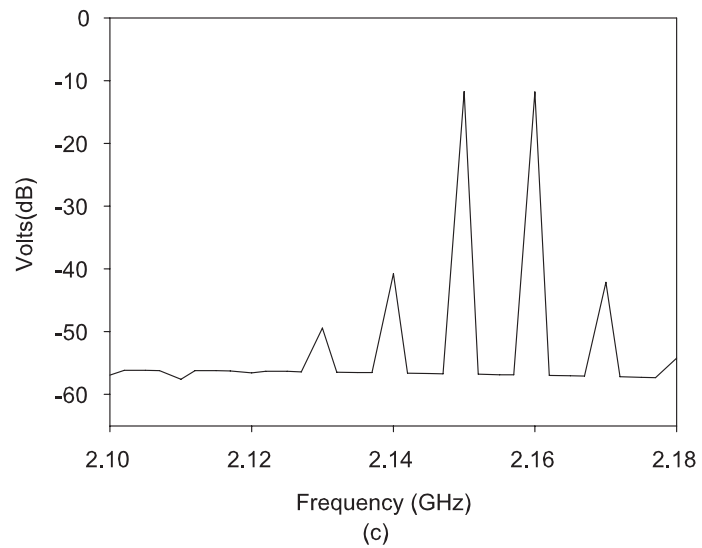


Figure 5.7: Comparison of original case and three optimized cases for the result of IIP3 response. A zoom-in plot for the operation frequency. Plots (a) is the original case, (b) is a maximization of the voltage gain, (c) is a minimization of the noise figure, and (d) satisfied all specifications.

5.3 Summary

In this chapter, we provide the constraints of the circuit parameters and the targets of the responses for the optimization. The seven responses are transformed into desirability function D , and we maximize the desirability function to get optimal recipes. Three cases of optimal recipes are obtained and the results all satisfy specifications . In Appendix A we give the completed contour plots. Finally we take the three cases of optimal recipes to run circuit simulator and compare with the original case.

